

Solving rescheduling problems in heterogeneous urban railway networks using hybrid quantum-classical approach

Mátyás Koniorczyk¹, Krzysztof Krawiec², Ludmila Botelho^{3,4},
Nikola Bešinović⁵, Krzysztof Domino³

¹HUN-REN Wigner Research Centre for Physics, Konkoly-Thege Miklós út 29-33., Budapest, 1121, Hungary.

²Faculty of Transport and Aviation Engineering, Silesian University of Technology, Akademicka 2A, Gliwice, 44-100, Poland.

³Institute of Theoretical and Applied Informatics, Polish Academy of Sciences, Bałycka 5, Gliwice, 44-100, Poland.

⁴Joint Doctoral School, Silesian University of Technology, Akademicka 2A, Gliwice, 44-100, Poland.

⁵“Friedrich List” Faculty of Transport and Traffic Sciences, Technical University of Dresden, Dresden, 01069, Germany.

Contributing authors: konioczyk.matyas@wigner.hun-ren.hu;
krzysztof.krawiec@polsl.pl; lbotelho@iitis.pl;
nikola.besinovic@tu-dresden.de; kdomino@iitis.pl;

We address the applicability of hybrid quantum-classical heuristics for practical railway rescheduling management problems. We build an integer linear model for the given problem and solve it with D-Wave’s quantum-classical hybrid solver as well as with CPLEX for comparison. The proposed approach is demonstrated on a real-life heterogeneous urban network in Poland, including both single- and multi-track segments and covers all the requirements posed by the operator of the network. The computational results demonstrate the readiness for application and benefits of quantum-classical hybrid solvers in the realistic railway scenario: they yield acceptable solutions on time, which is a critical requirement in a rescheduling situation. At the same time, the solutions that were obtained were feasible. Moreover, though they are probabilistic (heuristics) they offer a valid alternative by returning a range of possible solutions the

dispatcher can choose from. And, most importantly, they outperform classical solvers in some cases.

Keywords

railway rescheduling, conflict management, heterogeneous urban railway network, quantum annealing, hybrid quantum-classical heuristics

1 Introduction

Rail transport is expected to experience an increase in capacity demands due to changes in mobility needs resulting from climate policy, leading to traffic challenges in passenger and cargo rail transport. The situation is aggravated by the fact that the rolling stock and especially railway infrastructure cannot keep up with the increase in transport needs, which makes railway systems overloaded.

Rail transport, due to its technical and organizational characteristics is very sensitive to disturbances in traffic: these extraordinary events have an impact on railway operations, typically resulting in delays (Ge, Voß, & Xie, 2022). Examples of such disturbances include: late train departures/arrivals, extended dwell times, or (partial) track closures (also referred to as disruptions). These can last from several minutes up to hours. The impact of disturbances can propagate to multiple sections in the railway network (cf. the work of (Törnquist, 2007) and references therein). Thus, ensuring stable railway traffic and providing reliable service for passengers, rail cargo companies, and their clients is in the best common interest of railway infrastructure managers, and train operators. To limit these impacts as much as possible it is necessary to make proper rescheduling decisions quickly. The dispatchers need to reschedule and partially reroute the trains, aiming at the minimization of negative consequences. Still, in many places, dispatchers are using their own intuition or simple heuristics like FCFS (First Come First Served); resulting in decisions far from the objective of consequence minimization. In the last decades, there has been a growing research interest in mathematical optimization methods in support of rail dispatchers in decision making. While doing so, diverse objective functions were addressed, such as the (weighted) sum of delays (Lange & Werner, 2018), the maximal delay that cannot be avoided (D'Ariano, Pacciarelli, & Pranzo, 2007), or fuel consumption measures (Harrod, 2011).

As a railway network is a complex non-local structure, modeling a bigger portion of it is necessary for efficient suppression of the consequences of disturbances. Hence, large-scale rescheduling problems have to be addressed, and as the time available for making decisions is limited, they have to be solved almost real time. Therefore it is vital to develop efficient algorithms. However, the current conventional rescheduling optimization models have difficulties addressing complex and large-scale instances in suitable computation time (Caimi, Fuchsberger, Laumanns, & Lüthi, 2012; Lamorgese, Mannino, Pacciarelli, & Krasemann, 2018; Meng & Zhou, 2014).

The railway dispatching/rescheduling problem can broadly be recognized as being equivalent to job-shop scheduling with blocking and no-wait constraints (Mascis & Pacciarelli, 2002; Szpigiel, 1973). A possible modeling approach is based on alternative graphs employing order and precedence variables (Lange & Werner, 2018), facilitating

the formulation as a mixed integer linear program which is often large, hence, specialized algorithms are often used instead (D'Ariano et al., 2007; Lamorgese et al., 2018). An alternative approach is to use time-indexed models: discrete-time units and binary decision variables that assign events to particular time instants. Even though this results in very large problems, it is applied for both timetabling and dispatching/rescheduling (Caimi et al., 2012; Domino et al., 2023; Lusby, Larsen, Ehrgott, & Ryan, 2013; Meng & Zhou, 2014).

As time indexed models result in integer or 0-1 programs, they are suitable (Venturelli, Marchand, & Rojo, 2015) for to be solved on new types of hardware: quantum annealers (Apolloni, Carvalho, & De Falco, 1989; Kadowaki & Nishimori, 1998). These physical devices can be considered as stochastic heuristic solvers for Quadratic Unconstrained Binary Optimization (QUBO) problems, and there are few commercially available options, including D-Wave (Johnson et al., 2011). The exploration of their potential applications attracts a growing research interest (c.f. Section 2.2), in which railway applications are not yet strongly represented.

In this paper, we address the train rescheduling problem in complex railway networks with mixed infrastructure including single, double, and multiple track railway lines with given planned train paths. Our consideration includes shunting movement of rolling stock between depots and stations followed by rolling stock connections. We apply a new hybrid rescheduling algorithm combining classical-quantum modelling and based on Quantum Annealing (QA). This work extends on a particular linear modeling strategy, partly explored on a toy model in (Domino, Kundu, Salehi, & Krawiec, 2022). We develop an Integer Linear Programming (ILP) model, which is solved with proprietary D-Wave solvers as well as with CPLEX for comparison. The D-Wave approach is analysed in detail, with respect to its applicability and performance in a practically relevant situation. The results suggest that quantum computing and QA in particular, although an early-stage technology, are ready for tackling challenging railway rescheduling problems. During the preparation of the present work, another contribution has appeared in the literature (Xu et al., 2023), which is similar to our in that it sets up a QUBO model for a somewhat similar problem, and solves it by a simulation of (quantum) annealing. This contribution, however, considers a different railway infrastructure: high-speed trains, and considers timetable optimization, for which it employs a model different from the one described here.

The main contributions of the present work are the following:

- A railway traffic dispatching model is introduced for rescheduling trains due to disturbances and disruptions taking into account given timetable, rolling stock connections and a network with single or multi-track segments.
- QA-based hybrid heuristics are, for the first time, applied to real-life problems of railway rescheduling optimization on urban railway networks, these heuristics have some but still meaningfully input of real QA.
- The performance of the hybrid (quantum classical) D-Wave solver is demonstrated on a real-life network in Poland and diverse disturbance scenarios of different sizes and types.
- The D-Wave hybrid solver provides good quality solutions in short time, also for the complex instances in limited computational time.

- For certain instances the hybrid (quantum classical) D-Wave solver outperforms classical solvers in terms of computational time, yielding still feasible solutions.

The paper is organized as follows. In Section 2 we review state-of-the-art literature and identify scientific gaps we intend to fill, in Section 3 we describe problem under investigation, in Section 4 we evaluate our model, in Section 5 we discuss the hybrid solver we use, in Section 6 we present computational results.

2 Literature review

In this section, we present time-indexed models known from the literature, comparing them briefly with our modelling approach. For a general review of railway timetabling and rescheduling we refer to the reviews by (Lusby, Larsen, & Bull, 2018) and (Cacchiani et al., 2014). Second, we review recent QA applications in optimization in general, and also in the rail/transport domain. Finally, we summarize the existing scientific gaps.

2.1 Classical railway dispatching/rescheduling

Time-indexed modelling of railway scheduling and rescheduling is quite common in literature for routing (Caimi et al., 2012; Lusby et al., 2013) and scheduling (Caprara, Fischetti, & Toth, 2002; Dal Sasso, Lamorgese, Mannino, Onofri, & Ventura, 2021; Harrod, 2011; Meng & Zhou, 2014) . (Caimi et al., 2012) focus on determining train’s path for a complex central railway station area (called the blocking - stairway), used a discrete-time model resulting in a 0 – 1 program. Their model is successfully demonstrated on an operational day at the central railway station area Berne, Switzerland. Similarly, (Lusby et al., 2013) consider train movements in a single major (and thus complex) railway junction, including a freight yard and a few minor stations. They build a mixed integer programming model that can also be solved close to optimal in case of practically relevant instances. They address the train movements on the level of detail of acceleration and deceleration strategies, hence adopting a significantly finer discrete time scale than our one-minute resolution. When compared to our problem, these two models addressed a high traffic in a complex station area. Instead, we are concerned more with a bigger area, multiple stations, and mixed track, but a lower train density and complexity. Our train routes fixed within the stations, and we also model shunting movements that is not a subject of the cited reference.

(Caprara et al., 2002) proposed a graph theoretic formulation for the problem using a directed multigraph in which nodes correspond to departures/arrivals at a certain station at a given time instant. This formulation is used to derive an integer linear programming model that is solved using a Lagrangian relaxation. (Dal Sasso et al., 2021) introduced a new pure 0-1 programming formulation, and call it Tick Formulation, to model the Deadlock Detection (DD) problem. (Meng & Zhou, 2014) focused “on the train dispatching problem on an N-track network, with the main challenge of how to formulate specific retiming, reordering, retracking and rerouting options in combination”. Their model was demonstrated on generic networks of different structure than what we address. In our situation we are limited to retiming and reordering of trains.

Structurally, their model shows similarities to ours, including the role of binary variables and also the introduction of "cells" that generalize the objects the occupancy of which can be controlled: they can be one or more blocks, stations, etc. In our model, the decision variables will be explicitly linked to a subset of stations.

2.2 Quantum Annealing and its applications

Quantum Annealing (QA) (Das & Chakrabarti, 2008) is an optimization method analogous to Simulated Annealing (SA). Both can be used for the unconstrained minimization of a quadratic function of ± 1 -valued variables, which represents the energy configuration for a set of spins of the Ising model (Bian, Chudak, Macready, & Rose, 2010; Ising, 1925); an important and celebrated problem in physics. The Ising problem can be equivalently rewritten in a form of a Quadratic Unconstrained Binary Optimization (QUBO) problem with binary (0–1) variables. The Max-Cut problem (Boros & Hammer, 1991) is also equivalent to the Ising model or QUBO. The problem is NP-hard, has tremendous literature in classical optimization, and there is significant ongoing progress in the development of algorithms to solve it (Dunning, Gupta, & Silberholz, 2018; Gusmeroli et al., 2022). An extensive list of Ising problems and their formulations are presented e.g. in the work of (Lucas, 2014).

Hardware quantum annealers, like the D-Wave machine, implement a quantum version of the Ising model, assigning a quantum bit, i.e. a two-level physical quantum system to each bit. The system employs real physical two-level quantum systems with a tunable energy operator (Hamiltonian), the energy being the objective function of the optimization problem. An adiabatic evolution of the quantum system is implemented: the interactions between the spins are slowly changed from an initial Hamiltonian with a simple minimal-energy state to the Hamiltonian corresponding to the objective according to the rules of quantum mechanics. According to the adiabatic theorem of quantum mechanics (Avron & Elgart, 1999), under certain conditions the physical system remains in its lowest energy state during the evolution, and an optimal, minimum-energy solution can be possibly read out at the end.

An ideal adiabatic quantum computer would be a device with a large number of perfect quantum bits completely decoupled from their environment, very close to zero temperature. Any pair of qubits could be coupled, and even, more general couplings, e.g. involving 3 or more spins could take place. Such a system would exhibit perfect quantum coherence and entanglement. Even in such an ideal system the evolution time to reach at a minimum energy state with high enough probability is inverse proportional to the gap between the minimal energy configuration and the one closest to it. Certainly the gap is not known in advance, hence, the annealing time has to be determined by experimenting in practice. A more severe issue is that the gap can be very small, hence, it is not possible to solve all possible hard problems on such a setup. In spite of that, there are problems in which this approach can be efficient.

Meanwhile, the state-of-the-art physical quantum annealers are smaller systems of a few hundred quantum bits in which not all qubits are coupled, and the arrangement operates at a finite temperature. The fixed topology of qubit couplings means that the problem's graph defined by the nonzero coupling has to be embedded as

an induced subgraph of the topology of the system. This embedding is a hard problem itself (Zbinden, Bärtschi, Djidjev, & Eidenbenz, 2020). It often requires to couple multiple physical qubits to represent a logical bit of the problem. As for the finite temperature, the adiabatic evolution works also in systems that interact with their environment (Venuti, Albash, Lidar, & Zanardi, 2016). This introduces noise, whose impact, as discussed in detail by Albash, Martin-Mayor, and Hen (2017), increases with the system size.

Operationally, from the optimizer's point of view quantum annealers can be viewed as probabilistic heuristic solvers returning a statistical sample (Domino, Koniorczyk, & Puchała, 2022) of configurations which are supposed to be optimal or close to optimal. It must be stressed that the quantum annealers are not algorithms running on digital computers; they are analog devices implemented physically. This latter implies that the coefficients of the problem are encoded with a limited accuracy, and the algorithmic properties of the particular optimization problem such as its complexity class will not determine the solver's behaviour.

To overcome the problem of limited size and accuracy, quantum annealers of the present state of the art are often used in hybrid (quantum classical) solvers, orchestrating classical algorithms and using QA as a subroutine in order to address hard problem instances more efficiently. Solvers available in D-Wave's 'Leap Hybrid Solver Service (HSS)' (D-Wave Quantum Inc., 2022a), including the one used in the present work, belong to this family. Meanwhile, quantum technology keeps on developing, systems of bigger size and better topology are regularly announced, they are more and more affordable, and there is a growing community around them.

Currently, the applicability of QA technologies is being explored. Benchmark problems are solved (McLeod & Sasdelli, 2022; Willsch et al., 2022), comparisons with digital computers are made (Jünger et al., 2021), etc. The application of quantum annealers in transportation optimization is a new area with only a few contributions so far. There is an apparent interest in this research direction in the aviation domain (Stollenwerk, Lobe, & Jung, 2019; Stollenwerk et al., 2020; P.N. Tran, Pham, Goh, Alam, & Duong, 2020), which relates also to the already mentioned benchmarking of annealers as done by (Willsch et al., 2022). Shipment rerouting was also addressed in the context of QA (Yarkoni, Huck, et al., 2021). There are a few examples of hybrid solvers' applications, too. These include traffic flow optimization (Neukart et al., 2017), multi-car paint shop optimization (Yarkoni, Alekseyenko, et al., 2021), tail assignment problem (Martins, Rocha, & Castro, 2021), and vehicle optimization (Glos, Kundu, & Salehi, 2023).

In railway context, the first applications of QA can be found in train dispatching/rescheduling (Domino, Koniorczyk, Krawiec, Jałowiecki, & Gardas, 2021; Domino, Kundu, et al., 2022) and rolling stock planning (Grozea, Hans, Koch, Riehn, & Wolf, 2021). In particular, the first proof-of-concept demonstration of a (pure) quantum computing approach to railway rescheduling was presented by some of us (Domino et al., 2023). A followup paper (Domino, Kundu, et al., 2022) laid down the principles of a more general modeling approach to railway rescheduling in light of QA, introducing a suitable QUBO / HOBO (Higher-Order Binary Optimization) encoding of these problems. The present work continues this line of research.

2.3 Scientific gaps

We recognize several important scientific gaps. First, existing optimization models suffer from the curse of dimensionality, and inability to solve larger real-life instances. Second, the QA models for the studied optimization problem that have been introduced so far (Domino et al., 2021; Domino, Kundu, et al., 2022) had been designed for pure QA implementations and have been demonstrated only on simple network setups due to the size limitations of the currently available Noisy Intermediate Scale Quantum (NISQ) devices. Third, no hybrid QA-based models have been used for real-life railway, or even other schedule-based modes, like public transport and air traffic planning and/or rescheduling.

In this paper we demonstrate the quantum readiness of medium-scale railway rescheduling models: we successfully apply quantum methods in the rescheduling problem of a urban railway networks. To do so, we use a hybrid approach combining quantum and classical computing. For a fair comparison of current and future QA approaches with state-of-the-art classical approaches, we elaborate the railway model readily suitable for both classical and hybrid (quantum classical) solvers in a comparable manner. Quantum computing is believed to develop rapidly in near future. Hence, demonstration quantum readiness for railway problems right now is step forward towards the demonstration of quantum advantage in future. On future quantum devices the comparison with classical solvers is expected to be in strong favour for the quantum ones. In this way we also contribute in developing a novel general set of railway rescheduling models that has a potential to scale well with the size of the problem, aiming to overcome the curse of dimensionality.

3 Problem description

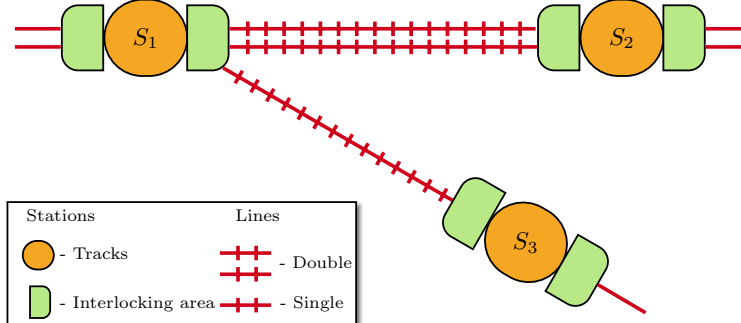


Fig. 1 Edges and nodes on the example railway network. Interlocking areas of stations in green.

We consider a railway rescheduling problem that includes train reordering, retiming, and shunting movements with rolling stock circulation at stations. Also, we consider an urban railway network with mixed tracks from single, double, up to quadruple tracks.

We model a railway network with edges and nodes of a graph. Figure 1 depicts an exemplary network layout composed of nodes (station or junction) and edges (single, double, multiple track lines). Each edge is composed of one or more *tracks*. Each track consists of blocks sections defined by pairs of signals (Lusby et al., 2013). Each block section can be occupied by at most one train at a time. A subsequent train is allowed to enter the block only after a minimal *headway*: minimal time span between the trains. We assume a 2-block signalling system, meaning that two free blocks are required between the consecutive trains. We also assume green way policy (trains have the free way to move at the maximal allowed speed between stations), resulting in constant running times for each block.

Each node is composed of station tracks (blocks) and interlocking areas. One station track can be occupied by one train at a time. Routing dependencies between pairs of trains competing for the same resource in interlocking areas are considered in order to guarantee that only one train from the pair can occupy the area at the time.

A train's *route* is the sequence of blocks the train passes during its journey. A train *path* is a sequence of arrival and departure times of a particular train assigned to a train route. We assume a one-minute resolution for all time parameters such as timetable time, running and dwell time minimal headway time or passing time, resulting in integer variables. This assumption of discretized time is needed to enable the use of quantum-based solvers, and, more importantly, introduces the possibility of pruning the inherently binary variables. The relaxation of integer constraints on time variables is not expected to improve computation time significantly, as the real difficulty is tied to precedence of trains, encoded later on precedence binary variables.

In the network, two trains can follow each other, i.e. keep the given order, meet and pass (M-P) when going the opposite directions, and meet and overtake (M-O), i.e. change the order, when going the same direction. Single tracks are designed for bidirectional traffic, double-tracks for unidirectional, one for each direction, and *multi-track* lines can be combination of unidirectional and bidirectional. On *single-track* lines, M-Ps and M-Os are only possible at stations. To prevent M-P on single-track lines, we determine the set $\mathcal{J}_{\text{single}}^2$ as the set of all pairs of trains that can potentially meet on the single track line heading in opposite directions.

Trains in the same direction preserve their order between stations, and keep the minimal headway time between each other. To prescribe these we determine set $\mathcal{J}_{\text{headway}}^2$: the set of all pairs of trains that can potentially violate the minimal headway condition.

The train traffic is scheduled on the basis of the given timetable. The timetable contains all the train paths. In the train rescheduling problem, we are given an initial timetable that is conflict-free. However, conflicts may appear due to disturbances such as late departures and/or arrivals due to excessive passenger demand, malfunctioning rolling stock, etc. Following (Corman, D'Ariano, Pacciarelli, & Pranzo, 2012), a *conflict* is an inadmissible situation when at least a pair of trains claim the same resource (e.g., block section, switch) simultaneously. We assume that the conflict may occur either on the railway line or at the station. Possible conflicts that can occur on the line include the lack of the minimum headway between two subsequent trains heading on the same track in the same direction, or claiming a segment of a single track line

by two trains heading in opposite directions at the same time. Conflicts at stations include claiming a station track by two trains at the same time, claiming a station switch (in the interlocking area) by two trains at the same time.

The conflicts have to be solved by modifying the original timetable, applying decisions on the train sequencing and retiming for trains claiming for the same resource. Such an intervention in the structure of train paths implies additional changes to maintain the feasibility of the modified timetable. These changes typically result in delays of additional trains that were not directly involved in the conflict otherwise, giving rise to *secondary delays* depending on the dispatching decision depending on the modification of the timetable. It is common in the literature to minimize a function of these secondary delays (see e.g. the work of (D'Ariano et al., 2007)); we will do this in the present contribution, too).

An important element of our approach is that from amongst all stations we first determine a subset of the *decision stations*; we assume that the direct decisions implied by our model affect these stations only. Hence, as decision stations we select those stations, where routes of trains intersect, where trains start or terminate, or where selected part network is bounded. The motivation is that if the routes of trains are fixed, the decisions on modifying their train paths has to be made with respect to these stations. (If we change some of the trains' routes in a re-routing process, new model with new parameters if developed, e.g. additional decision stations may appear.) In what follows, by a station we always mean a decision station. This also means that non-decision stations appear only through the parameter values in the model, they do not appear as indices of decision variables or parameters. Headways, for instance, are calculated between decision stations, taking into account all the line blocks and station blocks of non-decision stations in between.

On the station where a train terminates or sets off, shunting is also modeled. The goal of shunting is to move the train from the passengers' service track to the depot or vice versa. The depot is treated as the station, and consider it as a black box, without detailed layout. We treat shunting movements as service train from depot to the starting station of the service train, or from the terminating station to the depot. The rolling stock circulation condition is applied to ensure the precedence between the service train and the actual train.

In this way our model shares features of both microscopic and macroscopic models. At the *decision stations* it is microscopic as it takes into account station technology, track occupancy, rolling stock circulation, and shunting. Meanwhile from the point of view of the rest of the network it is a macroscopic model.

4 Methods and Model

In the following we describe our model in detail. Section 4.1 defines sets, parameters and decision variables. Section 4.2 describes our Integer Linear Programming (ILP) formulation.

4.1 Sets, parameters and decisions

To formulate our decision variables, constraints and the objective function, we determine sets of index tuples needed to find the actual index sets of variables, from the given infrastructure data, timetable data, and the rolling stock circulation plan. Also, we introduce parameters calculated from the same input.

4.1.1 Sets

Let us denote by \hat{S} the set of all stations, and by $S \subset \hat{S}$ the decision stations we have determined in advance, as already described. The main objects of our model for railway rescheduling are the trains $j \in \mathcal{J}$ and the stations $s \in \mathcal{S}_j$ in their path. Set \mathcal{S}_j includes decision stations only and it is an ordered set. In addition to \mathcal{J} and \mathcal{S}_j , the relevant sets are the following. Set $\mathcal{J}_s^{2(\text{turn})} \subset \mathcal{J} \times \mathcal{J} (\forall s \in S)$ is the set of all pairs of trains so that the first train of the pair terminates at station s and its rolling stock continues as the second train of the pair. This set is deduced from the rolling stock circulation plan and the timetable. Set $\mathcal{J}^{2(\text{close})} \subset \mathcal{J} \times \mathcal{J}$ is the set of trains which are close enough to each other in time so that precedence variables have to be defined for them. More details will be given at the description of the parameter d_{\max} which this set depends on. Set $\mathcal{J}^{2(\text{headway})} \subset \mathcal{J}^{2(\text{close})}$ is the set of train pairs that can potentially violate the minimal headway time between two subsequent trains on a line segment. For a pair of trains to be in $\mathcal{J}^{2(\text{headway})}$, both their routes need to include the same line segment so that the trains are moving in the same direction on it and can meet there according to model parameters, i.e. maximal allowed delay. Set $\mathcal{J}^{2(\text{single})} \subset \mathcal{J}^{2(\text{close})}$ is the set of all trains that share at least one single-track line segment as a common part of their routes so that they are heading in the opposite direction. Set $(\forall s \in S) \mathcal{J}_s^{2(\text{track})} \subset \mathcal{J}^{2(\text{close})}$ is the set of train pairs that are planned to occupy the same track on station s anytime during the planning horizon, thereby competing for the same track. Set $(\forall s \in S) \mathcal{J}_s^{2(\text{switch,out})} \subset \mathcal{J}^{2(\text{close})}$ is the set of train pairs that are planned to pass the same interlocking area of s upon their departure from station s . Set $(\forall (s, s') \in S^{\times 2}) \mathcal{J}_{s,s'}^{2(\text{switch,out,in})} \subset \mathcal{J}^{2(\text{close})}$ is the set of train pairs that are planned to pass the same interlocking area of s in order to have j to departure s while j' arrive s from the direction of s' . Set $(\forall s \in S^{\times 2}) \mathcal{J}_{s,s'}^{2(\text{switch,in,noMP})} \subset \mathcal{J}^{2(\text{close})}$ is the set of train pairs that are planned to pass the same interlocking area of s upon their arrival at s from the direction of s' , and there is no M-P possibility for them between s and s' . Set $(\forall s \in S^{\times 2}) \mathcal{J}_{s,s'}^{2(\text{switch,in,MP})} \subset \mathcal{J}^{2(\text{close})}$ is the set of train pairs that are planned to pass the same interlocking area of s upon their arrival at s so that either they both come from the direction of s' but there is a M-P possibility for them between s and s' , or one of them is approaching s from a direction other than s' . Set $(\forall j \in \mathcal{J}) \mathcal{C}_j^2$ is the set of all station pairs that are subsequent in the route of j . Set $(\forall (j, j') \in \mathcal{J}^{\times 2}) \mathcal{C}_{j,j'}^{2(\text{common})}$ is the set of all station pairs that appear as subsequent stations in the route of both j and j' heading in the same direction. Set $(\forall (j, j') \in \mathcal{J}^{\times 2}) \mathcal{C}_{j,j'}^{2(\text{common, single})}$ is the set of all station pairs that appear as subsequent stations in the route of both j and j' which are connected with a single-track line segment, and trains are heading in opposite directions. The order within the

pairs is determined by j . All these sets can be enumerated on the basis of the input data in a straightforward manner.

4.1.2 Parameters

The parameters that appear in our model are the following:

- $\tau^{(\text{pass})}(j, s \rightarrow s')$ is the running time of j from s to s' .
- $\tau^{(\text{headway})}(j, j', s \rightarrow s')$ is the minimal headway time for j' following j from s to s' .
- $\tau^{(\text{switch})}(j, j', s)$ is the running time of j over a interlocking area of s , where j may be in conflict with j' . (In our examples we do not consider cases when, e.g., on bigger stations there are multiple switches with different technological times. The model could trivially be extended to cover such scenarios by adding extra indices if relevant.)
- $\tau^{(\text{dwell})}(s, j)$ is the minimal dwell time of j at s .
- $\tau^{(\text{turn})}(s, j, j')$ is the minimum turnaround time for the rolling stock of a train j terminating at s to continue its journey as train j' .
- $\sigma(j, s)$ is the scheduled departure time of s from j , given by the original timetable.
- $v(j, s)$ is the earliest possible departure time of j from s when a disturbance and/or disruption in the network happens. It is the maximum of $\sigma(j, s)$ and the technically feasible earliest departure time, and may be more constraining than the first depending on the initial delays. The latter is calculated assuming that the train follows its planned route at minimum running time, and that there are no other trains present on the network.
- d_{\max} is an upper bound assumed for the secondary delay $t^{(\text{out})}(j, s) - v(j, s)$. This parameter sets an upper limit for the possible secondary delays that can arise on the particular part of the network. Setting such a bound is common in the literature, see e.g. the work of (D'Ariano et al., 2007). We set the same value of this parameter for all our testing instances. It has to be big enough so that no secondary delay exceeds it (e.g. $d_{\max} = 40$ excludes the possibility of a one-hour delay due to waiting for another delayed train). Meanwhile it is desirable to set its value as small as possible; restricting the time variables to small intervals decreases the number of binary decision variables in the model.

The choice of a small d_{\max} parameter results in a decrease of the model size, which is achieved via defining the set $J^2(\text{close})$. A pair of trains (j, j') is included in this set if and only if they can meet on any station, given the original timetable, the disturbed/disrupted timetable, and assuming that no train can have a secondary delay greater than d_{\max} . The number of constraints will be proportional to the average number of trains that can meet another train at a station; this will be linear in d_{\max} .

4.1.3 Decision variables

Our decision variables are the following. First, we use departure time variables:

$$t^{(\text{out})}(j, s) \in \mathbb{N} \quad (1)$$

defining the departure time of train $j \in \mathcal{J}$ from station $s \in \mathcal{S}_j$. Such a variable is defined for all decision stations \mathcal{S}_j . In the case of trains that terminate within the modeled part of the network, the last station is not included in \mathcal{S}_j . The arrival time of the trains at stations, $t^{(\text{in})}(j, s) \in \mathbb{N}$ are trivially related to the $t^{(\text{out})}(j, s)$ variables through a constant offset (c.f. Eq. (3)), given the fixed running time assumption.

Second, in addition to the time variables, we use three sets of binary precedence variables. Decision variables $y^{(\text{out})}(j, j', s) \in \{0, 1\}$ determine the order of trains to leave stations: the variable takes the value 1 if train j leaves station s before train j' , and 0 otherwise. The (j, j', s) tuples for which an y variable is defined will be specified later. Similarly, the precedence variables $y^{(\text{in})}(j, j', s) \in \{0, 1\}$ prescribe the order at the entry to stations; the value is 1 if j arrives to s before j' . The last set of precedence variables describes the precedence of trains at some resource located between stations s and s' (e.g. single track used by j and j' heading in opposite direction). The binary variable $z(j, j', s, s') \in \{0, 1\}$ will be 1 if j uses the given resource before j' . Also in this case, the quadruples (j, j', s, s') for which we have such a variable will be specified later.

4.2 ILP formulation

Given the index sets, variables, and the parameters and decision variables of the model, now we formulate the optimization objective and the constraints.

4.2.1 Objective function

Our goal is to minimize the secondary delays that occur in the analyzed part of the railway network. Hence, a suitable objective function is the *weighted sum of secondary delays at the destination station*:

$$f(t) = \frac{1}{d_{\max}} \sum_{j \in \mathcal{J}} w(j) \left(t^{(\text{out})}(j, s^*) - v(j, s^*) \right). \quad (2)$$

where s^* is the last element of S_j , and w_j are weights for each train representing its priority. The reason for restricting ourselves to the secondary delays at the destination stations only is that this is the actual figure of merit chosen by the respective railway authorities; the generalization to other linear objectives such as the weighted sum of secondary delays on all stations is straightforward. The constant multiplier $1/d_{\max}$ is optional; we use it for better comparability of different instances.

4.2.2 Constraints

The constraints of the model are the following.

Minimal running time

Each train needs a minimal time to get to the subsequent station:

$$\forall j \in \mathcal{J} \quad \forall (s, s') \in \mathcal{C}_j \quad t^{(\text{in})}(j, s') = t^{(\text{out})}(j, s) + \tau^{(\text{pass})}(j, s \rightarrow s') \quad (3)$$

Headways

A minimal headway time is required between subsequent train pairs on the common part of their route as

$$\forall(j, j') \in \mathcal{J}^2 \text{ (headway)} \quad \forall(s, s') \in \mathcal{C}_{j, j'}^2 \text{ (common)} \quad t^{(\text{out})}(j', s) \geq t^{(\text{out})}(j, s) + \tau^{(\text{headway})}(j, j', s \rightarrow s') - C \cdot y^{(\text{out})}(j', j, s), \quad (4)$$

where C is a constant big enough to make the constraint satisfied whenever the binary variable $y^{(\text{out})}(j', j, s)$ takes the value of 1. (Constraints of this structure are often termed as big-M constraints in this context.) In our implementation we calculate and use the smallest suitable value of C given particular d_{\max} value, i.e.

$$C = -\min(t^{(\text{out})}(j', s)) + \max(t^{(\text{out})}(j, s)) + \tau^{(\text{headway})}(j, j', s \rightarrow s') \quad (5)$$

Single-track occupancy

Trains moving in opposite directions cannot meet on the same single-track line segment:

$$\forall(j, j') \in \mathcal{J}^2 \text{ (single)} \quad \forall(s, s') \in \mathcal{C}_{j, j'}^2 \text{ (common, single)} \quad t^{(\text{out})}(j', s') \geq t^{(\text{in})}(j, s') - C \cdot z(j', j, s', s), \quad (6)$$

where C is a big enough constant chosen similarly to that in Eq. (4).

Minimal dwell time

Each train has to occupy the station node for a prescribed time duration at each station:

$$\forall j \in \mathcal{J} \forall s \in S_j \quad t^{(\text{out})}(j, s) \geq t^{(\text{in})}(j, s) + \tau^{(\text{dwell})}(j, s). \quad (7)$$

Timetable

No train is allowed to depart before its scheduled departure time:

$$\forall j \in \mathcal{J} \forall s \in S_j \quad t^{(\text{out})}(j, s) \geq \sigma(j, s). \quad (8)$$

Station track occupancy

Station tracks can be occupied by at most one train at a time:

$$\forall s \in S \forall(j, j') \in \mathcal{J}_s^2 \text{ (track)} \quad t^{(\text{in})}(j', s) \geq t^{(\text{out})}(j, s) - C \cdot y^{(\text{out})}(j', j, s), \quad (9)$$

where C is chosen similarly to that in Eq. (4) again. Note that this requirement may not be needed for depot tracks; the exceptions can be handled by the proper definition of \mathcal{J}_s^2 .

Interlocking area occupancy

These ensure that trains cannot meet in interlocking areas:

$$\begin{aligned} \forall s \in S \forall (j, j') \in \mathcal{J}_s^2 & \text{ (switch,out)} t^{(\text{out})}(j', s) \geq \\ t^{(\text{out})}(j, s) + \tau^{(\text{switch})}(j, j', s) - C \cdot y^{(\text{out})}(j', j, s), \end{aligned} \quad (10)$$

$$\begin{aligned} \forall (s, s') \in S^{\times 2} \forall (j, j') \in \mathcal{J}_{s, s'}^2 & \text{ (switch,out,in)} t^{(\text{in})}(j', s) \geq \\ t^{(\text{out})}(j, s) + \tau^{(\text{switch})}(j, j', s) - C \cdot z(j', j, s', s), \end{aligned} \quad (11)$$

$$\begin{aligned} \forall (s, s') \in S^{\times 2} \forall (j, j') \in \mathcal{J}_{s, s'}^2 & \text{ (switch,in,noMP)} t^{(\text{in})}(j', s) \geq \\ t^{(\text{in})}(j, s) + \tau^{(\text{switch})}(j, j', s) - C \cdot y^{(\text{out})}(j', j, s'), \end{aligned} \quad (12)$$

$$\begin{aligned} \forall (s, s') \in S^{\times 2} \forall (j, j') \in \mathcal{J}_{s, s'}^2 & \text{ (switch,in,MP)} t^{(\text{in})}(j', s) \geq \\ t^{(\text{in})}(j, s) + \tau^{(\text{switch})}(j, j', s) - C \cdot y^{(\text{in})}(j', j, s), \end{aligned} \quad (13)$$

with a choice of C similar again to that in Eq. (4).

Rolling stock circulation constraints

These are introduced in order to bind the train with the shunting movement called also service train. If the train set of train j which terminates at s is supposed to continue its trip as (service train) j' or vice versa, a precedence of these trains including a minimum turnaround time has to be ensured:

$$\forall s \in S \forall (j, j') \in \mathcal{J}_s^2 t^{(\text{out})}(j', s) \geq t^{(\text{in})}(j, s) + \tau^{(\text{turn})}(j, j', s). \quad (14)$$

Order of trains

We have additional conditions on the y -variables, concerning the case when M-O is not possible on the line or station.

$$\begin{aligned} \forall (j, j') \in \mathcal{J}^2 & \text{ (headway)} \forall (s, s') \in \mathcal{C}_{j, j'}^2 \text{ (common)} \\ \forall (j, j') \in \mathcal{J}^2 & \text{ (headway)} \cap \mathcal{J}_{s'}^2 \text{ (track)} \\ y^{(\text{out})}(j, j', s) &= y^{(\text{out})}(j, j', s') \end{aligned} \quad (15)$$

$$\begin{aligned} \forall (s, s') \in S^{\times 2} \forall (j, j') \in \mathcal{J}_{s, s'}^2 & \text{ (switch,in,MP)} \cap \mathcal{J}_{s'}^2 \text{ (track)} \\ y^{(\text{in})}(j, j', s') &= y^{(\text{out})}(j, j', s') \end{aligned}$$

The objective function in Eq. (2), together with the constraints in Eq. (3)-(14) define our mathematical programming model.

The model yields an integer linear program, and the time variables can be constrained even into a finite range using the parameter d_{\max} . Note that the binary variables have the obvious symmetry property

$$\begin{aligned} y^{(\text{out})}(j', j, s) &= 1 - y^{(\text{out})}(j, j', s) \\ z(j', j, s', s) &= 1 - z(j, j', s, s'), \end{aligned} \quad (16)$$

which is taken into account explicitly by using independent binary variables only.

As for the scaling of our model, the number of time variables i.e. $\#t$ is bounded by number of trains times number of stations $\#\mathcal{J}\#\mathcal{S}$ (see also Section 3.1 of the work of (Domino, Kundu, et al., 2022)). In order to obtain a more accurate estimate of the number of these variables we observe that in our model no trains visit all stations. We assume that in average each train visits $\alpha \in (0, 1)$ fraction of the stations, we have then

$$\#(t) \approx \alpha \#\mathcal{J}\#\mathcal{S}. \quad (17)$$

as a tighter bound.

Suppose, that most of the network is composed mainly of double track lines. Then there will be typically a single precedence variable per train and station ($y^{(out)}(j, j', s)$), and thus their number can be estimated by:

$$\#y + \#z \approx \#y \approx \alpha N(d_{\max}) \#\mathcal{J}\#\mathcal{S}, \quad (18)$$

where $N(d_{\max})$ is number of trains the train can meet at a station on average. Under such assumptions the total number of variables grows linearly with number of trains and stations:

$$\#vars = \#t + \#y + \#z \approx \text{const} \#\mathcal{J}\#\mathcal{S}. \quad (19)$$

If, on the other hand, the network has dominantly single track lines, two precedence variables per train and station ($y^{(out)}(j, j', s)$ and $z(j, j', s, s')$) will be needed, and thus

$$\#y = \#z \approx \alpha N(d_{\max}) \#\mathcal{J}\#\mathcal{S}. \quad (20)$$

In both cases we assume that there are not many ($y^{(in)}(j, j', s)$) variables, as they are tied certain particular interlocking area conditions.

Based on Eq. (16) there are typically 2 constraints per each y variable as headway and station track occupation constraints, and 2 constraints per each z variable as single track occupation constraints. For the interlocking area occupation constraints it is more complicated as it involves both z and y variables; a good assumption is to consider 2 constraints for each y variable. For the running time and minimal dwell time we expect one constraint per train and station. Thus number of constraints can be estimated by

$$\#constr. \approx 6\#y + 2\#z + 2\#\mathcal{J}\#\mathcal{S} \quad (21)$$

where the second term is tied to single track line conditions (one condition per z variable).

$$\#constr. \approx \begin{cases} \alpha(6N(d_{\max}) + 2)\#\mathcal{J}\#\mathcal{S} & \text{for double track} \\ \alpha(8N(d_{\max}) + 2)\#\mathcal{J}\#\mathcal{S} & \text{for single track.} \end{cases} \quad (22)$$

Because of the limitations in time imposed by d_{\max} the model can be viewed as linear in number of trains and number of stations. Hence, as expected, the model is more complex for the network in which single track lines dominate. Although the analysed network is mostly composed of the double track lines, we will analyse certain use-cases with the fraction of single track lines increased.

Observe that without limiting the secondary delays by d_{\max} , the value of $N(d_{\max})$ would only be bounded by $\#\mathcal{J} - 1$ (as each train is considered to possibly meet each other), which would result in quadratic scaling of the number of precedence variables and number of constraints in the number of trains.

5 Hybrid quantum-based approach

To overcome the limitations described in in Section II of current hardware quantum annealers, we apply hybrid (quantum classical) solver. In particular, we use the 'Leap Hybrid Solver Service (HSS)' ([D-Wave Quantum Inc., 2022a](#)); a cloud-based proprietary solver which is developed by the market leader of QA hardware and is available as a service. It utilizes a hybrid approach that combines classical computational power with quantum processing.

In particular, we have used the Constrained Quadratic Model (CQM) ([D-Wave Quantum Inc., 2022b](#)) Solver. The CQM hybrid solver works as follows.

Input

A constrained linear or quadratic model, and the value of the solver parameter `t_min`, which prescribes the minimum required run time (in seconds) solver is allowed to work on any problem.

Preprocessing

Preprocessing includes subproblem identification and decomposition to smaller instances ([T. Tran et al., 2016](#)). Furthermore, the solver's internal preprocessing mechanism takes constraints into account automatically, implementing the suitable penalty method internally.

Processing

The hybrid solver implements a workflow that combines a portfolio of various classical heuristics (including tabu search, simulated annealing, etc.) running on powerful CPUs (Central Processing Units) and GPUs (Graphics Processing Units). In the course of the solution process the hardware quantum annealer is also invoked, in order to solve smaller QUBO problems that can potentially boost the classical heuristics. Integer problems are transformed to binary using state-of-the-art methods like the one described by ([Glover, Kochenberger, & Du, 2019](#)) ([Karimi & Ronagh, 2019](#)), generally applicable for integer problems. When using the quantum hardware, the solver performs the required embedding, runs the QUBO subproblem on the physical QA device several times, and returns a sample of potential solutions. After these readouts, the sample is incorporated into the solution workflow. In this way, even though the physical annealer supports problems with limited size (e.g. the Pegasus machine has 5500 physical qubits ([Dattani, Szalay, & Chancellor, 2019](#)), and several of these may be needed to represent a binary variable because of the embedding), the approximate solutions of small subproblems contribute to the solution process. The final solution is composed by the solver's module.

Output

The solution of the integer or quadratic constrained problem. The workflow results in a solution that is not guaranteed to be optimal, hence, the hybrid solver as a whole is in nature a heuristic solver. Furthermore, the solver is probabilistic, hence each at each run the final solution may be different.

While D-Wave's proprietary solvers act as black boxes, i.e. they hide the exact details of the described process from the user, the output is supplemented with timing parameters, including *run time*: the total elapsed time including system overhead, and *Quantum Processing Unit (QPU) access time* which is the time spent accessing the actual quantum hardware. These parameters enable a comparison with other solvers.

As mentioned before, in addition to the actual problem to be solved, the CQM solver optionally inputs another parameter, t_{\min} . This is a time limit for heuristics running in parallel (D-Wave Quantum Inc., 2022b): unless a thread does not terminate by itself after t_{\min} , it is allowed to run at least till t_{\min} before it is stopped at the current best solution. We have sampled the CQM problems with various settings of t_{\min} and uncovered the impact of this setting to the model performance and solution quality for our problem.

The CQM Solver can solve problems encoded in the form of Eq. (2) – (15) (c.f. Section 4.2) with up to 5000 binary or integer variables and 100,000 constraints. Computational results of railway rescheduling problems were obtained using classical as well as hybrid (quantum classical) solvers. As a classical solver, IBM ILOG CPLEX Interactive Optimizer (version 22.1.0.0) was used. The CPLEX computation was performed on 16 cores of *Intel(R) Core(TM) i7-10700kF CPU 3.80GHz* with 64GBs of memory. As hybrid solver, the D-Wave CQM hybrid solver (version: 1.12) was used.

6 Computational results

In this section, we demonstrate the performance of the proposed hybrid (quantum classical) approach on a network at Polish railways - central part of the Upper Silesia Metropolis. In particular, we compare the performance of D-Wave's hybrid quantum-classical solver (CQM) with CPLEX. The comparison is performed for diverse network layouts including single-, double-, and multiple-track lines, and different level of disturbances and disruptions including various initial delays and track closures. As the objective is tied to secondary delays, we can roughly apply it to assess the degree of difficulty of the problem.

Section 6.1 describes the considered network and traffic characteristics. Section 6.2 presents results concerning generic examples on the core line of the network, comparing double track line scenarios with single track line scenarios and closure scenarios. Section 6.3 presents analogous results for larger network with real-life timetable. Here the case studies concerns various scenarios with different degree of difficulty.

6.1 Railway network

We use the Open Railway Map¹ representation of the selected part of the Polish railway network located in the central part of the Metropolis GZM (Poland), presented in Fig 2. The selected part of the network combines heterogeneous network layout including single-, double-, triple-, and quadruple-track lines. It comprises 25 nodes including 11 stations and 3 junctions, 146 blocks, and 2 depots. The infrastructure is managed by Polish state infrastructure manager PKP PLK (Polskie Koleje Państwowe, Polskie Linie Kolejowe eng. Polish State Railways, Polish Railway Lines).

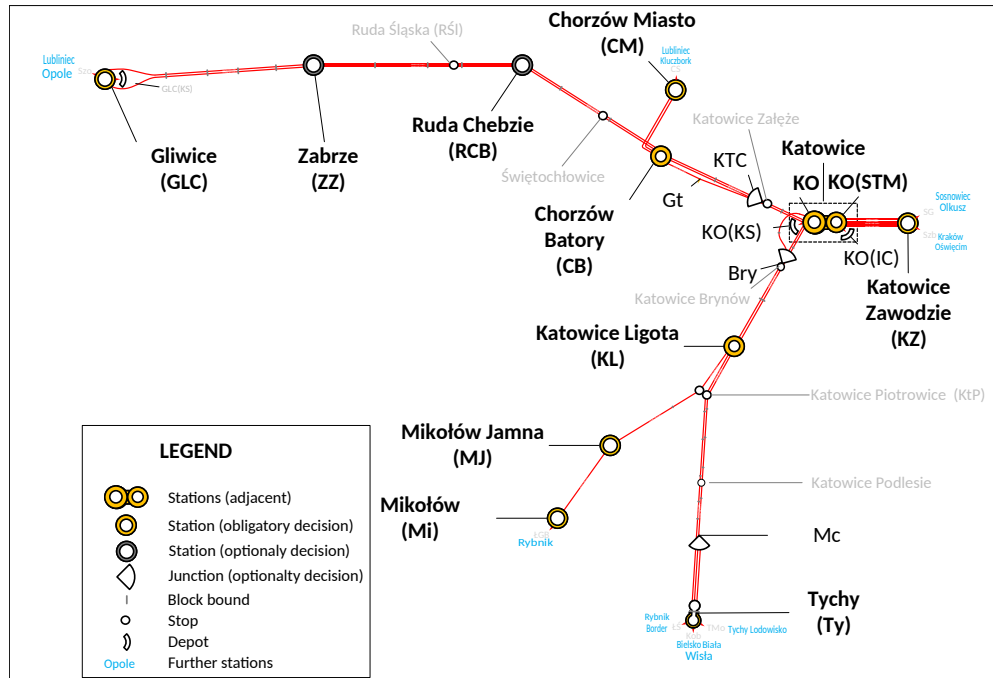


Fig. 2 Selected part of Polish railway network located in the central part of the Metropolis and examined in our research.

The decision stations include stations $\{KO, KO(STM), CB, KL\}$, stations bounding the analysed part of the network $\{GLC, CM, KZ, Ty, Mi\}$, depots $\{KO(KS), KO(IC)\}$ from which regional and intercity trains are being shunted to and from $\{KO\}$, and stations on the single track line – $\{MJ\}$ to allow meet and pass (M-P) or meet and overtake (M-O). As described before, the decision stations are the only ones that appear explicitly in our model. Due to operational reasons resulting from track design, the decisions on train departure times (and thus on trains' order) are, in the current operational practice, *de facto* made with respect to the decision stations. All other stations and junctions are treated as line blocks as long as no rerouting or retracking

¹ <https://www.openrailwaymap.org/>, visited 2022-11-25

is considered; they will appear in the model implicitly via parameters. These stations include:

- stations $\{\text{ZZ}, \text{CB}\}$ in which usually there are rigid assignments of the platform tracks to the traffic direction (i.e., track 1 towards $\{\text{GLC}\}$; track 2 towards $\{\text{KO}\}$)
- branch junctions $\{\text{KTC}, \text{Bry}, \text{Mc}\}$ in which usually there is a rigid assignment to the tracks.

As an example, let for a particular train j , $\hat{\mathcal{S}}_j = \{\text{KZ}, \text{KO(STM)}, \text{KO}, \text{KTC}, \text{CB}, \text{RCB}, \text{ZZ}, \text{GLC}\}$ be the ordered set of stations. Then, the dispatching decisions *de facto* affect directly the *decision stations* $\mathcal{S}_j = \{\text{KZ}, \text{KO(STM)}, \text{KO}, \text{CB}, \text{GLC}\}$. The set of decision stations can be extended if necessary.

In all computation priority weights in Eq. (2) we use $w_j = 1$ for stopping (local) trains $w_j = 1.5$ for intercity (fast) trains $w_j = 1.75$ for express trains, and $w_j = 0$ for shunting (if applicable). As for the solver parameter t_min , after initial experiments we have decided to prefer $\text{t_min} = 5\text{s}$ as it provides a good balance between computation time and expected solution quality. Sensitivity analysis regarding this parameter is performed in Appendix A for selected instances.

6.2 Synthetic experiments on the selected railway line

As the first set of experiments we address, synthetic instances on a part of the network - railway line KO-GLC, see Fig 2. The goal in these scenarios is to compare the CPLEX and CQM solvers for: the double track line (*line1*), the double track line with closures (*line2*), and the single track line (*line3*). Shunting movements and rolling stock circulation are not considered in this set of experiments. In particular, the addressed configurations are the following:

1. *Line1*, the double track line with dense traffic. We use cyclic 3-hour timetable with 10 trains each hour and each direction, i.e. we have 59 trains.
2. *Line2*, similar to *line1*, with the additional closure of one of the tracks between ZZ and RCB. We use a cyclic 2-hour timetable with 10 trains each hour and each direction, i.e. we have 40 trains.
3. *Line3*, the whole line is considered as a single track, with a timetable of 3 hours traffic and 21 trains.

For *line1* and *line3*, the original timetable is feasible, while for *line2* it is not feasible due to the closure. For each of the lines we compute 12 instances, each with different initial delays of trains subsets. Instance 0 yields no initial delays. Thereafter, we use the parameter value $d_{\max} = 40\text{ min}$, in all cases in this and subsequent subsection. Assuming that each train interacts with $N(d_{\max}) = 12$ trains for *line1* and *line2*, and with $N(d_{\max}) = 6$ trains for *line3*, Eqs. (17) - (19), (22) allows us to quickly estimate the sizes of the problem. This sizes are compared with computed (comp.) actual number of variables and constraints (mean over instances) in Tab. 1. Here, *line2* is the most complex in terms of constraints, what is reflected later by computational difficulties of some of its instances. Furthermore, *line2* is partially double track and partially single track, hence the actual number of constraints is bounded from above

| 1 | # S | # \mathcal{J} | # int vars | | # precedence vars | | # constraints | |
|---|-------|-----------------|------------|----------|-------------------|----------------------------------|---------------|-------------------------|
| | | | comp. mean | Eq. (17) | act. mean | Eq. (18)/Eq. (20) doub./sing. | comp. mean | Eq. (22) doub./sing. |
| 1 | 3 | 59 | 118 | 118 | 1538 | 1415 / - | 7889 | 8731 / - |
| 2 | 5 | 40 | 142 | 133 | 1394 | 1600/3200 | 8491 | 6867/13067 |
| 3 | 5 | 21 | 79 | 70 | 592 | - / 840 | 3057 | - / 3499 |

Table 1 Synthetic experiments. The first column is the ordinal number of the line. For the estimated and actual number of variables and constraints, we use $\alpha = 2/3$ in Eqs. (17) - (19), (22) (doub. - double track, sing. - single track, comp. mean - computed actual number of variables or constraints, mean over instances).

by the estimate for the single track line and from below by the estimate for the double track line. *Line1* includes double-, whereas *line3* single-track segments only. There actual number of constraints and variables appeared to be close to the estimate.

The computational results are presented in Figs. 3, 4, and 5 for *line1*, *line2*, and *line3*, respectively. Each figure shows objective $\times d_{\max}$ (top part), computation time (comp. time, middle part) and QPU access time (bottom part) for CQM hybrid solver with t_{\min} equal 5 and 20s. CPLEX results are also displayed.

For scenario *line1* (Fig. 3), CQM solver obtained optimal solutions for all cases (except for instances 6 and 11). Similarly, for *line3* (Fig. 5), only small deviations from the optimum can be observed for a number of instances. All computational times for *line1* and *line3* were significantly below 0.4min, although CPLEX performed faster. Comparing CQM with $t_{\min} = 5s$ and $t_{\min} = 20s$, we have almost the same objectives but $t_{\min} = 20s$ requires almost 4 times longer computational time.

For *line2* (Fig. 4), all CQM solutions were suboptimal, although feasible. More remarkably, for 9 instances at $t_{\min} = 5s$ and 3 instances at $t_{\min} = 20s$ (out of 12 instances) CQM was faster than CPLEX, in several cases up to 5 \times faster. This difference in time is clear while setting the minimal processing time of the CQM solver $t_{\min} = 5s$ (see Section 5). This observation is approved by more detailed discussion on t_{\min} parameter in Appendix A. In principle, *line1* (Fig. 3) and *line3* (Fig. 5) are less complicated in terms of number of constraints, and here solutions of CPLEX and CQM are similar in terms of objective, but CPLEX is faster. We can conclude that the utility of the CQM solver can be expected for the more complex instances of railway scheduling problems.

6.3 Real-life experiments on the considered rail network

In this subsection, we will test the CQM solver on more realistic scenarios of the railway traffic on presented network. We will also focus on the track closure situation, turning a double track line segment into a single track one, under dense traffic, to elaborate our findings from *line2* in Section 6.2. Our computations address various use cases of train delays outside the network and within the network as well as the partial track closure. We constructed 9 networks with increased level of difficulty ranging from small delays to disruptions, i.e. it is expected more trains are involved and/or disturbances are spread more over the network. These networks are tabulated in Table 2. Their details are as follows:

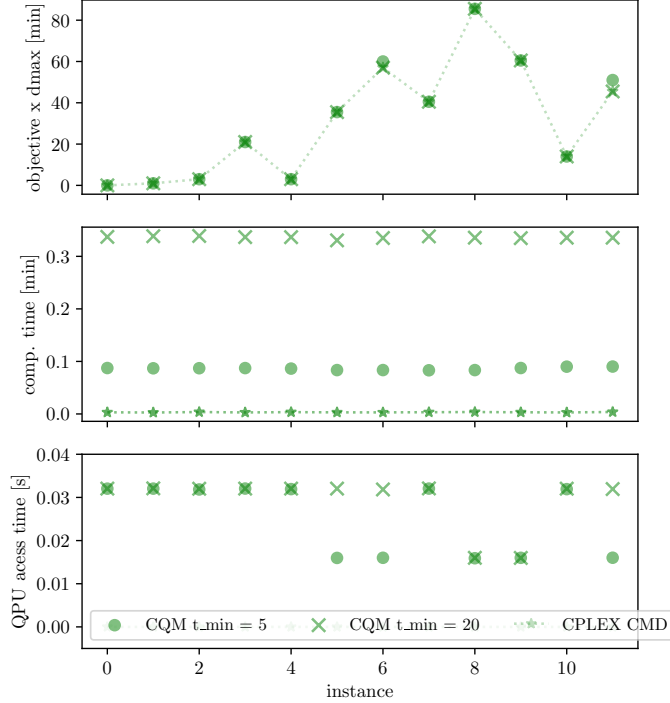


Fig. 3 Synthetic experiments *Line1*, comparison of the performance of classical solver (CPLEX) with that of the hybrid CQM. All the displayed solutions are feasible. Total computational time (middle panel) and QPU times (lower panel) were provided by the D-Wave output. Results of both solvers were similar in terms of the objective, but the CPLEX computation was faster.

1. Networks 1 - 3 concern only disturbances due to delayed trains and no closures.
2. Networks with number 4 or higher concern also disturbances due to closures.
 - (a) Networks 4 and 5 concerns rerouting trains from double track line KTC-CB to the single track line with higher passing times, see Fig. 2 (trains have no initial delays in network 3 and some initial delays in network 4).
 - (b) Network 6 concerns multiple closures, i.e. change of multiple line KZ-KO(STM) and double track line KO-KL to single track lines. (See Fig. 2; the reason can be e.g. upcoming reconstruction works on this part of network.)
 - (c) Networks 7 - 9 concerns closures of both 5 and 6, but each with different initial delays of trains. The intention of the last 3 networks is to create a really challenging rescheduling problem.
3. For comparison, network 0 is the default problem with no disturbances.

Table 3 tabulates the results comparing CPLEX and CQM in terms of objective function value and computation time; problem sizes and QPU times are included. As CQM is probabilistic, 5 runs have been performed for each network, yielding 5 different realizations. This also facilitates the analysis of the statistics of the output and the differences between particular realizations.

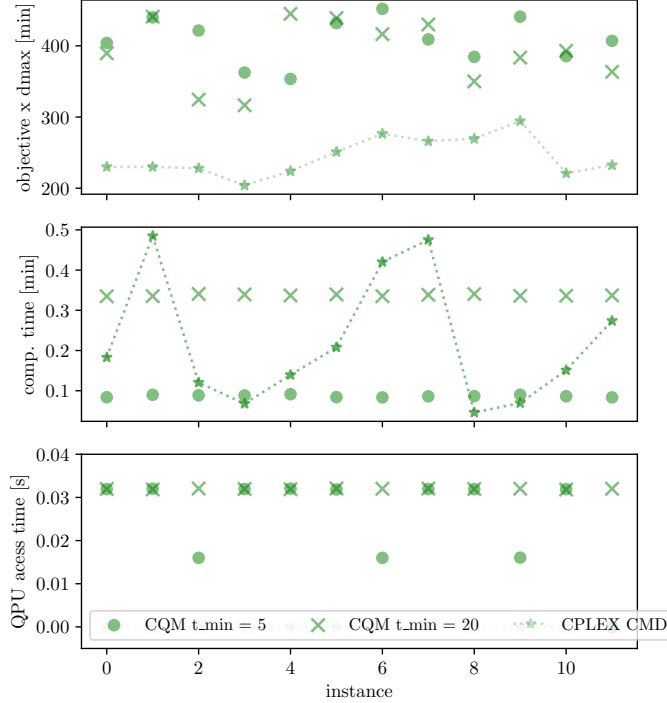


Fig. 4 Synthetic experiments *Line2*, comparison of the performance of classical solver (CPLEX) with that of the hybrid CQM. Note that the CQM is fast, even when compared to CPLEX. The found solutions are suboptimal but can be useful. All the displayed solutions are feasible. *Line2*, namely the double track line with closures and dense traffic, has appeared to be most challenging for both the classical solvers (in terms of computational time) and for the quantum solver (in terms of objective). On this example, there are instances, where the current CQM D-Wave hybrid solver outperforms CPLEX in terms of computational time. Increasing the value of the t_{\min} parameter in most cases improves the quality of the solution at the cost of computational time.

The level of difficulty increases with respect to the number of variables and constraints. Observe that CQM always returns a feasible solution. For the networks 0 – 3 with initial delays only, CQM generated optimal solutions, while in the remaining networks, the objective value was somewhat higher than the actual optima obtained with CPLEX. As for computational times, for CPLEX they grow significantly - from 0.072 to almost 8s (network 9). Meanwhile those of CQM remain almost constant around 5.1s. QPU times remain not greater than 0.032s. Remarkably, for the hardest instances: networks 7 and 9, the CQM hybrid solver even outperforms CPLEX with respect to computational time. It does not find the actual optimum, just a feasible solution close to it. For example, in network 9, the computed CQM solution is around 30% worse than the optimal one. In conclusion, we expect benefits from the application of the hybrid solver on medium scale railway networks with multiple closures, as in networks 7-9. This is in accordance with our observation on synthetic data in Fig. 4, where the benefits appeared for more complex instances, too.

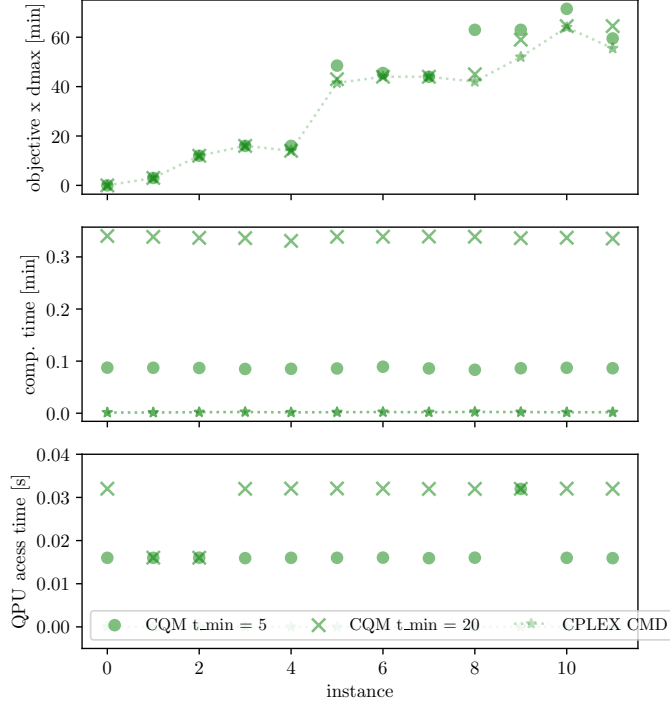


Fig. 5 Synthetic experiments *Line3*, comparison of the performance of classical solvers (CPLEX) with that of the hybrid CQM. All the displayed solutions are feasible. Results of both solvers were similar in terms of the objective, but CPLEX computation was faster.

To evaluate the extent of difficulty of the problems analysed in Tab. 3, Tab. 4 presents mean (over stations and realizations) delays, resulting from CQM solutions, on selected stations (i.e. stations in central part of the network in Fig. 2). Meaningful delays are introduced starting from network 4 onward, i.e. for networks with closures in a limited number of stations, see also Tab. 2. From network 5 onward, delays become more uniformly distributed among the stations when compared with results in Tab. 2. However, for networks 7 - 9 the mean delays are the highest and almost uniformly distributed among all stations, showing that the spread of disruption impacts the whole network. These have appeared to be more challenging network disruptions.

Fig. 6 shows more detailed statistical analysis for two networks 4 and 7 and compares CPLEX (top panel) vs CQM (bottom panel). For network 4 (left panel of Fig. 6), bigger delays occur mainly at stations KO(STM), KO and CB for both CPLEX and CQM solutions, albeit for the former are somewhat smaller. This reflects the initial disturbances, which indeed occurred mainly between KO and CB (see Tab. 2), and thus the spread is limited to these 3 stations. For network 7 (right panel of Fig. 6), delays are more spread through the network due to disruption and initial disturbances. To

| network | #S | place | trains involved | description |
|--|----|---------------|---|---|
| A. Disturbtions from outside the network | | | | |
| 1 | 10 | KO-Ty | IC 14006 KS 94113 | Delayed IC (higher priority) is in conflict with on-time KS |
| 2 | 10 | arr. Ty | KS 94766 KS 40518 IC 41004 KS 44862 IC 4120 | Delayed 5 trains on the arrival to Ty, random delays of several minutes |
| B. Disturbtions originated within the network | | | | |
| 3 | 10 | whole network | 14 trains KS + IC | Random delays of 14 trains delays up to 35 minutes |
| C. Disturbtions within the network and closures | | | | |
| 4 | 11 | KTC-CB | 10 trains KS + IC | Double track line KTC-CB closed trains rerouted to single track line |
| 5 | 11 | whole network | most trains | Double track line KTC-CB closed as in 4 + delays as in 3 |
| 6 | 10 | whole network | all trains | Multiple track KZ - KO(STM) and double track KO - KL changed into single track + delays as in 3 |
| 7 | 11 | whole network | all trains | Multiple track KZ - KO(STM) and double track KO - KL changed into single track + double track line KTC-CB closed as in 4 + delays as in 3 |
| 8 | 11 | whole network | all trains | Closures as in 7 + random delays of 13 trains up to 30 minutes |
| 9 | 11 | whole network | all trains | Closures as in 7 + random delays of 15 trains up to 30 minutes |

Table 2 Real-life experiments. Networks of particular dispatching problems. In networks 0 - 5 most of analysed network is double tracked, from network 6 upward the number of single track lines in the network increases at the expense of the number of double and multiple track lines. For each network we considered a two-hour time with an afternoon rush-hour timetable from the year 2021, with $\#J = 27$ trains. Beside the $\#S$ stations there are 2 depots in each network.

conclude, we can expect advantage from a hybrid (quantum classical) approach particularly in case of more complex problems with extensive disruptions and disturbances occurring throughout the whole network.

In order to further evaluate the solutions, we present time-distance diagrams for network 7, for the CPLEX solution and two different quantum realizations; these can be seen in Figs. 7, 8, and 9, respectively. We have chosen the line segment between GLC and KZ, offering a good demonstration. (We have introduced a small artificial 'distance' between KO and KO(STM) which are contiguous locations for sake of better visibility, hence the horizontal lines in the diagram.) The red dotted lines represent the conflicted situation, and the green solid lines represent the solution. All the three proposed solutions have similar figures of merit, they all provide a valid option to be realized. The conflicts are resolved in somewhat different ways, see e.g. the paths of trains 40150, 5312, and 26103. In details:

- in the CPLEX solution, train 26103 passes first the KTC-CB closure heading for GLC, then 40150 followed by 5312 go in opposite directions,
- in the CQM solution, first realization, 40150 and 5312 pass first the KTC-CB closure and 26103 waits at KTC for them to pass,

| n. | CPLEX | | | CQM hyb. $t_{\min} = 5$ s mean value over 5 realis. | | | comparison CQM vs. CPLEX | |
|----|----------------------|-----------------------|-------------------|--|-------------------|-----------------|-----------------------------|-------------------|
| | #vars / # constr. | obj. \times dmax | comp. time [s] | obj. \times dmax | comp. time [s] | QPU time [s] | obj. diff. % | comp t. diff % |
| 0 | 556 / 1756 | 0.0 | 0.07 | 0.0 | 5.19 | 0.03 | 0 % | - |
| 1 | 556 / 1756 | 1.0 | 0.08 | 1.0 | 5.24 | 0.02 | 0 % | - |
| 2 | 556 / 1740 | 6.0 | 0.08 | 6.0 | 5.37 | 0.03 | 0 % | - |
| 3 | 556 / 1769 | 7.5 | 0.09 | 7.5 | 5.05 | 0.03 | 0 % | - |
| 4 | 662 / 2210 | 78.25 | 0.20 | 82.70 | 5.10 | 0.03 | -5.6 % | - |
| 5 | 662 / 2204 | 114.75 | 0.25 | 132.55 | 5.25 | 0.02 | -15.5 % | - |
| 6 | 711 / 2599 | 91.25 | 0.41 | 142.3 | 5.14 | 0.03 | -55.9 % | - |
| 7 | 817 / 3029 | 188.75 | 7.98 | 263.4 | 5.12 | 0.02 | -39.5 % | 35.8 % |
| 8 | 817 / 3074 | 157.75 | 3.70 | 271.65 | 5.12 | 0.02 | -72.2 % | -38.4 % |
| 9 | 817 / 3081 | 185.5 | 6.51 | 263.85 | 5.11 | 0.02 | -42.2 % | 21.5 % |

Table 3 Real-life experiments. Results of ILP optimization on CPLEX and CQM D-Wave hybrid solver. $d_{\max} = 40$ was set for all networks. Computational times and QPU time were reported in D-Wave's output. We have selected $t_{\min} = 5$ s as it provides the best balance between computational time and the quality of solution. For detailed analysis see Appendix A. This appendix shows a detailed analysis of the impact of t_{\min} on computation time and solution quality for two specific real-life lines 7 and 9. The last columns present a percentage comparison (CQM - CPLEX) / CPLEX, hence, the positive values represent CQM advantage, whereas negative values show CPLEX advantage.

| network | Delay [min] | | | | |
|---------|-------------|------|------|------|-----|
| | KO(STM) | KO | CB | KL | MJ |
| 0 | 3.7 | 1.0 | 1.7 | 1.5 | 0.0 |
| 1 | 3.1 | 1.3 | 2.1 | 1.5 | 0.0 |
| 2 | 3.8 | 1.3 | 2.0 | 1.3 | 2.0 |
| 3 | 2.6 | 2.1 | 1.4 | 0.7 | 1.5 |
| 4 | 6.6 | 4.4 | 7.4 | 1.6 | 0.0 |
| 5 | 7.1 | 6.2 | 10.7 | 1.0 | 2.7 |
| 6 | 6.7 | 6.7 | 3.2 | 8.7 | 4.1 |
| 7 | 9.8 | 10.7 | 12.5 | 9.5 | 9.9 |
| 8 | 10.4 | 10.5 | 10.0 | 10.5 | 7.6 |
| 9 | 10.0 | 10.3 | 11.5 | 9.8 | 9.6 |

Table 4 Real-life experiments. Mean (over trains and realizations) secondary delay resulted from CQM solutions (Tab. 3) for all networks in Tab. 2. Non-zero values for network 0 comes from counted delays in shunting movement in KO and KO(STM) that are not included in the objective, as well as some cases where the train gets a few minutes delay but make it up and leaves the network on time - these are typical issues for the railway traffic on analysed network.

- in the CQM solution, second realization, 26103 passes first KTC-CB closure, then 5312 followed by 40150 go in opposite directions.

This results in following objective $\times d_{\max}$ values: for CPLEX - 188.75, for CQM first realization - 279 for CQM second realization - 261.5. Although, the first solution is optimal, it is reasonable to supply dispatchers with the range feasible solutions.

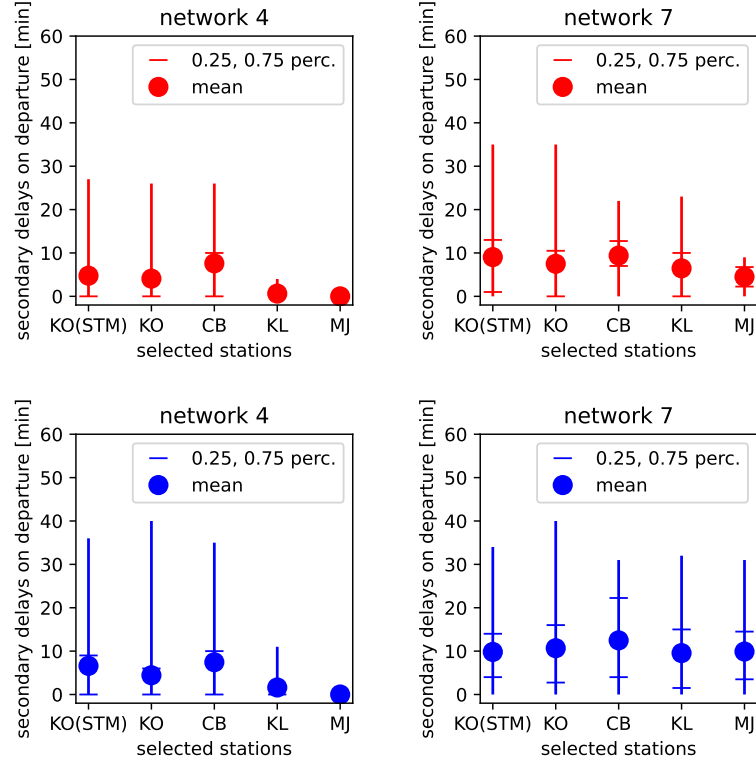


Fig. 6 Real-life experiments. Statistics of CPLEX (top panel) and CQM (bottom panel) solutions (Tab. 3) for selected networks in Tab. 2. The statistics were calculated over trains in the classical cases, and over trains and realizations in the CQM cases. Vertical lines are ranges, while horizontal lines are 0.25 and 0.75 percentiles.

Hence, these diagrams proved that CQM hybrid solver can produce usable solutions for railway traffic management.

An additional benefit of the probabilistic nature of the quantum-based method is that it produces different alternatives after each realization run without any modification. These could be offered to the dispatcher in a decision support system as possibilities. The dispatcher's choice can be influenced by other circumstances not covered by the present model.

7 Conclusions

We have demonstrated that quantum annealers can be readily applicable in train rescheduling optimization in urban railway networks. In particular we have encoded rescheduling problems in a linear integer program, and solved these using a state-of-the-art solver (CPLEX), as well as on the QA based CQM hybrid (quantum classical) solver. While the CQM hybrid solver does not outperform classical solvers in general, we have found specific cases in which they were actually better. This supports

the expectation that future quantum devices will be efficient in solving large scale-problems, and in our case, real-time railway dispatching problems on the national scale; even in the range that are beyond the scope of current exact models and heuristics.

While the quantum-based solvers would possibly return suboptimal solutions, these are still often better than the solutions obtained manually or based on smaller scale models. More importantly, all generated solutions were feasible. In each computation, the CQM hybrid solver always has taken some advantage of the QPU. Hence, we believe that such a little help from the QPU must have boosted the classical heuristics in the hybrid solver.

Recall that quantum annealer devices are subjects of many ongoing debates. Previous studies claimed that the quantum nature of their operation is limited (Shin, Smith, Smolin, & Vazirani, 2014), while recent works argue that their operation relies more on the thermalization with a cold environment in place of actual quantum adiabatic evolution (Buffoni & Campisi, 2020). They are often criticized for the small size of problems they can address and various classical solvers do outperform them on certain problems at the present state of the art. In spite of all these, our computational results demonstrate the readiness of hybrid (quantum classical) solvers to handle real-life railway problems. We believe that future investigations shall focus on hybrid approaches both for railway applications as well as more generally.

Finally, several future research directions can be determined. First concerns the ongoing worldwide works on the development of fault tolerant quantum computing devices (DiVincenzo, 2000) with proper error correction/mitigation, this will boost results of approaches supported by quantum computing (and QA in particular). Second concerns creation of custom open source hybrid solver that is dedicated for railway problems and will use noise of quantum device to our advantage e.g. by modelling some stochastic behaviour on railways. Third concerns evolution and application of quantum inspired techniques such as tensor networks technique, simulated bifurcation (Goto, 2019). With all these future developments, QA-based approaches tend to become more powerful and ready to address for the first time large-scale real-time challenges in railway traffic management, which are currently unsolvable with traditional techniques.

Data availability

The code and the data used for generating the numerical results can be found in https://github.com/iitis/railways_dispatching_silesia under DOI 10.5281/zenodo.10657323

Acknowledgements

This research was supported by the Ministry of Culture and Innovation and the National Research, Development and Innovation Office within the Quantum Information National Laboratory of Hungary (Grant No. 2022-2.1.1-NL-2022-00004) (MK), and by the Silesian University of Technology Rector's Grant no. BKM - 720/RT2/2023 12/020/BKM_2023/0252 (KK). This research was funded in part by National Science Center, Poland, under grant number 2019/33/B/ST6/0201 (LB) and

2023/07/X/ST6/00396 (KD). For the purpose of Open Access, the authors has applied a CC-BY public copyright licence to any Author Accepted Manuscript (AAM) version arising from this submission.

We would like to thank to Sebastian Deffner as well as to the whole scientific community of the Department of Physics, University of Maryland, Baltimore County (UMBC) for valuable discussion; and to Bartłomiej Gardas, and Zbigniew Puchała for valuable motivation; and to Katarzyna Gawlak, Akash Kundu, and Özlem Salehi for data validation and assistance with coding. We acknowledge the cooperation with Koleje Śląskie sp. z o.o. (eng. Silesian Railways).

Compliance with ethical standards

Conflict of interest

The authors declare that they have no conflict of interest.

Ethical approval

This article does not contain any studies with human participants or animals performed by any of the authors.

References

Albash, T., Martin-Mayor, V., Hen, I. (2017). Temperature scaling law for quantum annealing optimizers. *Physical Review Letters*, 119(11), 110502,

Apolloni, B., Carvalho, C., De Falco, D. (1989). Quantum stochastic optimization. *Stochastic Processes and their Applications*, 33(2), 233–244,

Avron, J.E., & Elgart, A. (1999, 01). Adiabatic theorem without a gap condition. *Commun. Math. Phys.*, 203(2), 445–463,

Bian, Z., Chudak, F., Macready, W.G., Rose, G. (2010). *The Ising model: teaching an old problem new tricks*. Retrieved from https://www.dwavesys.com/media/vbklsvh/weightedmaxsat_v2.pdf (visited 2022.04.29.)

Boros, E., & Hammer, P.L. (1991). The Max-Cut problem and quadratic 0–1 optimization; polyhedral aspects, relaxations and bounds. *Annals of Operations Research*, 33(3), 151–180,

Buffoni, L., & Campisi, M. (2020, jun). Thermodynamics of a quantum annealer. *Quantum Sci. Technol.*, 5(3), 035013,

Cacchiani, V., Huisman, D., Kidd, M., Kroon, L., Toth, P., Veelenturf, L., Wagenaar, J. (2014). An overview of recovery models and algorithms for real-time railway rescheduling. *Transportation Research Part B: Methodological*, 63, 15–37,

Caimi, G., Fuchsberger, M., Laumanns, M., Lüthi, M. (2012). A model predictive control approach for discrete-time rescheduling in complex central railway station areas. *Computers & Operations Research*, 39(11), 2578-2593,

Caprara, A., Fischetti, M., Toth, P. (2002). Modeling and solving the train timetabling problem. *Operations Research*, 50(5), 851–861,

Corman, F., D'Ariano, A., Pacciarelli, D., Pranzo, M. (2012). Bi-objective conflict detection and resolution in railway traffic management. *Transportation Research Part C: Emerging Technologies*, 20(1), 79-94, (Special issue on Optimization in Public Transport+ISTT2011)

D-Wave Quantum Inc. (2022a). *D-Wave Hybrid Solver Service: An Overview [WhitePaper]*. Retrieved from https://www.dwavesys.com/media/4bnpi53x/14-1039a-b_d-wave_hybrid_solver_service_an_overview.pdf (visited 2022.04.29.)

D-Wave Quantum Inc. (2022b). *Hybrid Solver for Constrained Quadratic Model [WhitePaper]*. Retrieved from https://www.dwavesys.com/media/rldh2ghw/14-1055a-a_hybrid_solver_for_constrained_quadratic_models.pdf (visited 2022.04.29.)

Dal Sasso, V., Lamorgese, L., Mannino, C., Onofri, A., Ventura, P. (2021). The tick formulation for deadlock detection and avoidance in railways traffic control. *Journal of Rail Transport Planning & Management*, 17, 100239,

D'Ariano, A., Pacciarelli, D., Pranzo, M. (2007). A branch and bound algorithm for scheduling trains in a railway network. *European Journal of Operational Research*, 183(2), 643-657,

Das, A., & Chakrabarti, B.K. (2008, September). *Colloquium : Quantum annealing and analog quantum computation*. *Reviews of Modern Physics*, 80(3), 1061–1081,

Dattani, N., Szalay, S., Chancellor, N. (2019, Jan). Pegasus: The second connectivity graph for large-scale quantum annealing hardware.

[arXiv:1901.07636](https://arxiv.org/abs/1901.07636) [quant-ph]

DiVincenzo, D.P. (2000). The physical implementation of quantum computation. *Fortschritte der Physik: Progress of Physics*, 48(9-11), 771–783,

Domino, K., Koniorczyk, M., Krawiec, K., Jałowiecki, K., Deffner, S., Gardas, B. (2023). Quantum annealing in the NISQ era: railway conflict management. *Entropy*, 25(2), 191,

Domino, K., Koniorczyk, M., Krawiec, K., Jałowiecki, K., Gardas, B. (2021). Quantum computing approach to railway dispatching and conflict management optimization on single-track railway lines. [arXiv:2010.08227](https://arxiv.org/abs/2010.08227) [cs.ET]

Domino, K., Koniorczyk, M., Puchała, Z. (2022). Statistical quality assessment of ising-based annealer outputs. *Quantum Information Processing*, 21(8), 288,

Domino, K., Kundu, A., Salehi, Ö., Krawiec, K. (2022). Quadratic and higher-order unconstrained binary optimization of railway rescheduling for quantum computing. *Quantum Information Processing*, 21(9), 1–33,

Dunning, I., Gupta, S., Silberholz, J. (2018, aug). What Works Best When? A Systematic Evaluation of Heuristics for Max-Cut and QUBO. *INFORMS Journal on Computing*, 30(3), 608–624,

Ge, L., Voß, S., Xie, L. (2022, Jun 04). Robustness and disturbances in public transport. *Public Transport*, 14, 191-261,

Glos, A., Kundu, A., Salehi, Ö. (2023). Optimizing the production of test vehicles using hybrid constrained quantum annealing. *SN Computer Science*, 4(5), 609,

Glover, F., Kochenberger, G., Du, Y. (2019). Quantum bridge analytics i: a tutorial on formulating and using qubo models. *4or*, 17, 335–371,

Goto, H. (2019). Quantum computation based on quantum adiabatic bifurcations of Kerr-nonlinear parametric oscillators. *Journal of the Physical Society of Japan*, 88(6), 061015,

Grozea, C., Hans, R., Koch, M., Riehn, C., Wolf, A. (2021, Sep). Optimising rolling stock planning including maintenance with constraint programming and quantum annealing. [arXiv:2109.07212v1](https://arxiv.org/abs/2109.07212v1) [cs.AI]

Gusmeroli, N., Hrga, T., Lužar, B., Povh, J., Siebenhofer, M., Wiegele, A. (2022, jun). BiqBin: A parallel branch-and-bound solver for binary quadratic problems with linear constraints. *ACM Trans. Math. Softw.*, 48(2), 1–31,

Harrod, S. (2011). Modeling network transition constraints with hypergraphs. *Transportation Science*, 45(1), 81–97,

Ising, E. (1925, feb). Beitrag zur theorie des ferromagnetismus. *Z. Physik*, 31(1), 253–258,

Johnson, M.W., Amin, M.H., Gildert, S., Lanting, T., Hamze, F., Dickson, N., ... others (2011). Quantum annealing with manufactured spins. *Nature*, 473(7346), 194–198,

Jünger, M., Lobe, E., Mutzel, P., Reinelt, G., Rendl, F., Rinaldi, G., Stollenwerk, T. (2021, dec). Quantum annealing versus digital computing. *ACM Journal of Experimental Algorithmics*, 26, 1–30,

Kadowaki, T., & Nishimori, H. (1998). Quantum annealing in the transverse Ising model. *Physical Review E*, 58(5), 5355,

Karimi, S., & Ronagh, P. (2019). Practical integer-to-binary mapping for quantum annealers. *Quantum Information Processing*, 18(4), 1–24,

Lamorgese, L., Mannino, C., Pacciarelli, D., Krasemann, J.T. (2018). Train dispatching. In R. Borndörfer, T. Klug, L. Lamorgese, C. Mannino, M. Reuther, & T. Schlechte (Eds.), *Handbook of Optimization in the Railway Industry* (pp. 265–283). Cham: Springer International Publishing.

Lange, J., & Werner, F. (2018). Approaches to modeling train scheduling problems as job-shop problems with blocking constraints. *Journal of Scheduling*, 21(2), 191–207,

Lucas, A. (2014). Ising formulations of many NP problems. *Frontiers in Physics*, 2, 5,

Lusby, R.M., Larsen, J., Bull, S. (2018). A survey on robustness in railway planning. *European Journal of Operational Research*, 266(1), 1–15,

Lusby, R.M., Larsen, J., Ehrgott, M., Ryan, D.M. (2013). A set packing inspired method for real-time junction train routing. *Computers & Operations Research*, 40(3), 713–724,

Martins, L.N., Rocha, A.P., Castro, A.J. (2021). A QUBO Model to the Tail Assignment Problem. *Icaart (2)* (pp. 899–906).

Mascis, A., & Pacciarelli, D. (2002). Job-shop scheduling with blocking and no-wait constraints. *European Journal of Operational Research*, 143(3), 498–517,

McLeod, C.R., & Sasdelli, M. (2022). Benchmarking D-Wave Quantum Annealers: Spectral Gap Scaling of Maximum Cardinality Matching Problems. *Computational science – ICCS 2022* (pp. 150–163). Springer International Publishing.

Meng, L., & Zhou, X. (2014). Simultaneous train rerouting and rescheduling on an n-track network: A model reformulation with network-based cumulative flow variables. *Transportation Research Part B: Methodological*, 67, 208–234,

Neukart, F., Compostella, G., Seidel, C., von Dollen, D., Yarkoni, S., Parney, B. (2017, December). Traffic flow optimization using a quantum annealer. *Frontiers in ICT*, 4, , <https://doi.org/10.3389/fict.2017.00029> Retrieved from <http://dx.doi.org/10.3389/fict.2017.00029>

Shin, S.W., Smith, G., Smolin, J.A., Vazirani, U. (2014, Jan). How "quantum" is the D-Wave machine? [arXiv:1401.7087v2](https://arxiv.org/abs/1401.7087v2) [quant-ph]

Soriani, A., Nazé, P., Bonança, M.V., Gardas, B., Deffner, S. (2022). Three phases of quantum annealing: Fast, slow, and very slow. *Physical Review A*, 105(4), 042423,

Stollenwerk, T., Lobe, E., Jung, M. (2019). Flight Gate Assignment with a Quantum Annealer. S. Feld & C. Linnhoff-Popien (Eds.), *Quantum technology and optimization problems* (pp. 99–110). Cham: Springer International Publishing.

Stollenwerk, T., O’Gorman, B., Venturelli, D., Mandrà, S., Rodionova, O., Ng, H., ... Biswas, R. (2020). Quantum annealing applied to de-conflicting optimal trajectories for air traffic management. *IEEE Transactions on Intelligent Transportation Systems*, 21(1), 285–297,

Szpigel, B. (1973). Optimal train scheduling on a single line railway. *Operational Research*, 72, 343–352,

Törnquist, J. (2007). Railway traffic disturbance management—An experimental analysis of disturbance complexity, management objectives and limitations in planning horizon. *Transportation Research Part A: Policy and Practice*, 41(3), 249–266,

Tran, P.N., Pham, D.-T., Goh, S.K., Alam, S., Duong, V. (2020, jun). An Interactive Conflict Solver for Learning Air Traffic Conflict Resolutions. *Journal of Aerospace Information Systems*, 17(6), 271–277,

Tran, T., Do, M., Rieffel, E., Frank, J., Wang, Z., O’Gorman, B., ... Beck, J. (2016). A hybrid quantum-classical approach to solving scheduling problems. *Proceedings of the international symposium on combinatorial search* (Vol. 7, pp. 98–106).

Venturelli, D., Marchand, D.J.J., Rojo, G. (2015). Quantum annealing implementation of job-shop scheduling.
[arXiv:1506.08479](https://arxiv.org/abs/1506.08479)

Venuti, L.C., Albash, T., Lidar, D.A., Zanardi, P. (2016, Mar). Adiabaticity in open quantum systems. *Phys. Rev. A*, 93, 032118,

Willsch, D., Willsch, M., Calaza, C.D.G., Jin, F., Raedt, H.D., Svensson, M., Michielsen, K. (2022, apr). Benchmarking advantage and D-Wave 2000q quantum annealers with exact cover problems. *Quantum Inf Process*, 21(4), ,

Xu, H.-Z., Chen, J.-H., Zhang, X.-C., Lu, T.-E., Gao, T.-Z., Wen, K., Ma, Y. (2023). High-speed train timetable optimization based on space–time network model and quantum simulator. *Quantum Information Processing*, 22(11), 418,

Yarkoni, S., Alekseyenko, A., Streif, M., Von Dollen, D., Neukart, F., Bäck, T. (2021). Multi-car paint shop optimization with quantum annealing. *2021 ieee international conference on quantum computing and engineering (qce)* (pp. 35–41).

Yarkoni, S., Huck, A., Schülldorf, H., Speitkamp, B., Tabrizi, M.S., Leib, M., ... Neukart, F. (2021). Solving the shipment rerouting problem with quantum optimization techniques. M. Mes, E. Lalla-Ruiz, & S. Voß (Eds.), *Computational logistics* (pp. 502–517). Cham: Springer International Publishing.

Zbinden, S., Bärtschi, A., Djidjev, H., Eidenbenz, S. (2020). Embedding Algorithms for Quantum Annealers with Chimera and Pegasus Connection Topologies. *International conference on high performance computing* (pp. 187–206).

Appendix A. Comparative analyses for different values of the t_{\min} parameter on selected solutions

The right choice of the t_{\min} parameter can improve results meaningfully. Hence, in this Appendix we analyse in more detail the role of the t_{\min} solver parameter for selected problems in Section 6.3. In particular, for networks 7 and 9 therein, we have performed runs with t_{\min} sweeping over a range [5, 60]; the results are presented in Fig. 10 and Fig. 11. The objective value is roughly log-linear in computational time. For small t_{\min} parameter values the computational time is shorter, whereas for large t_{\min} it grows exponentially. Overall, the improvement in the objective is overwhelmed by the increase of the computational time. This is important from the point of view of the algorithm layout, as it may be tied to a power law scaling. Such a behaviour is plausible in the case of QA methods (Albash et al., 2017; Domino, Koniorczyk, & Puchała, 2022; Soriani, Nazé, Bonança, Gardas, & Deffner, 2022).

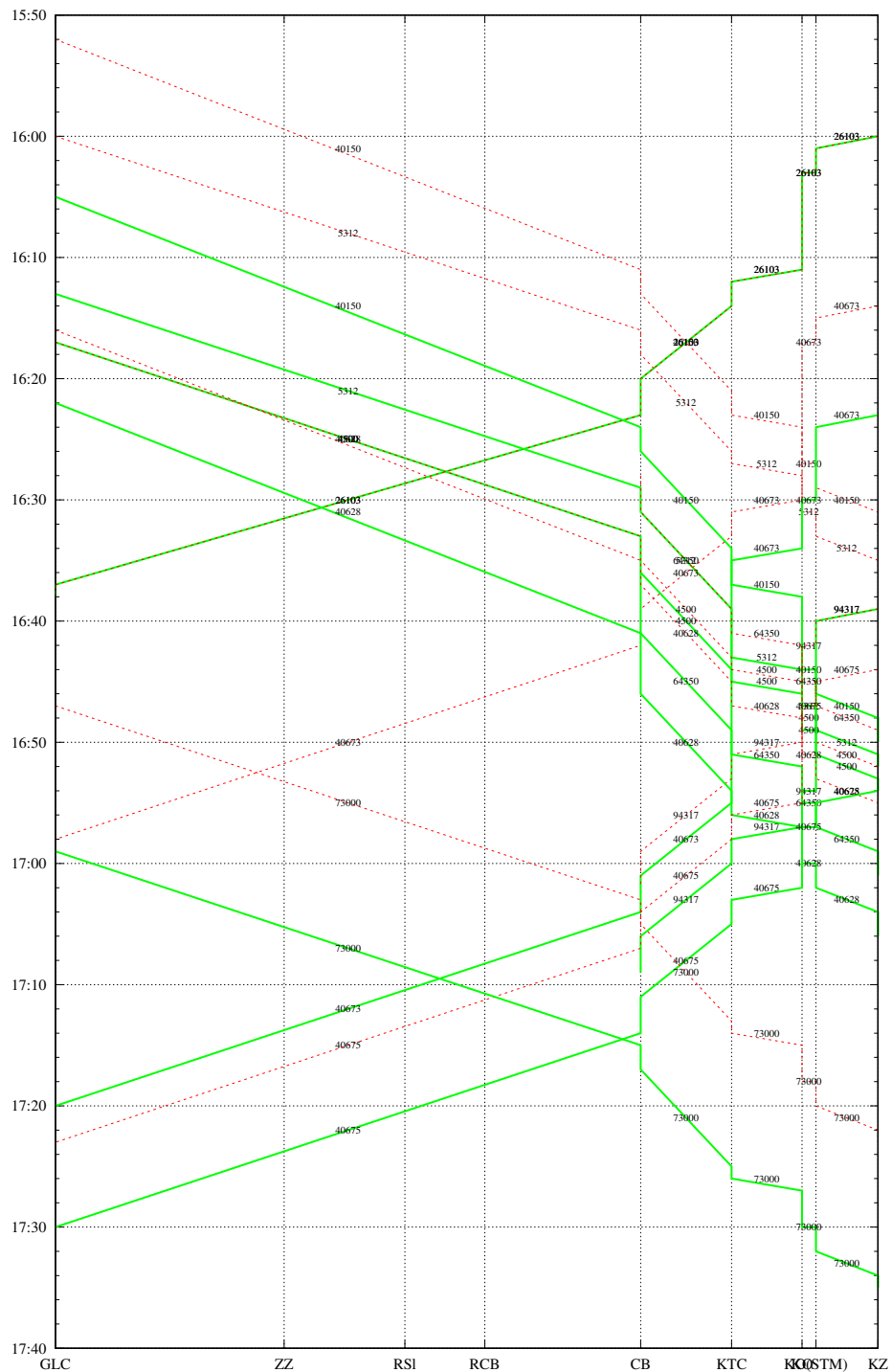


Fig. 7 Real-life experiment. Time-distance diagram CPLEX solution of network 7, see Tab. 2.

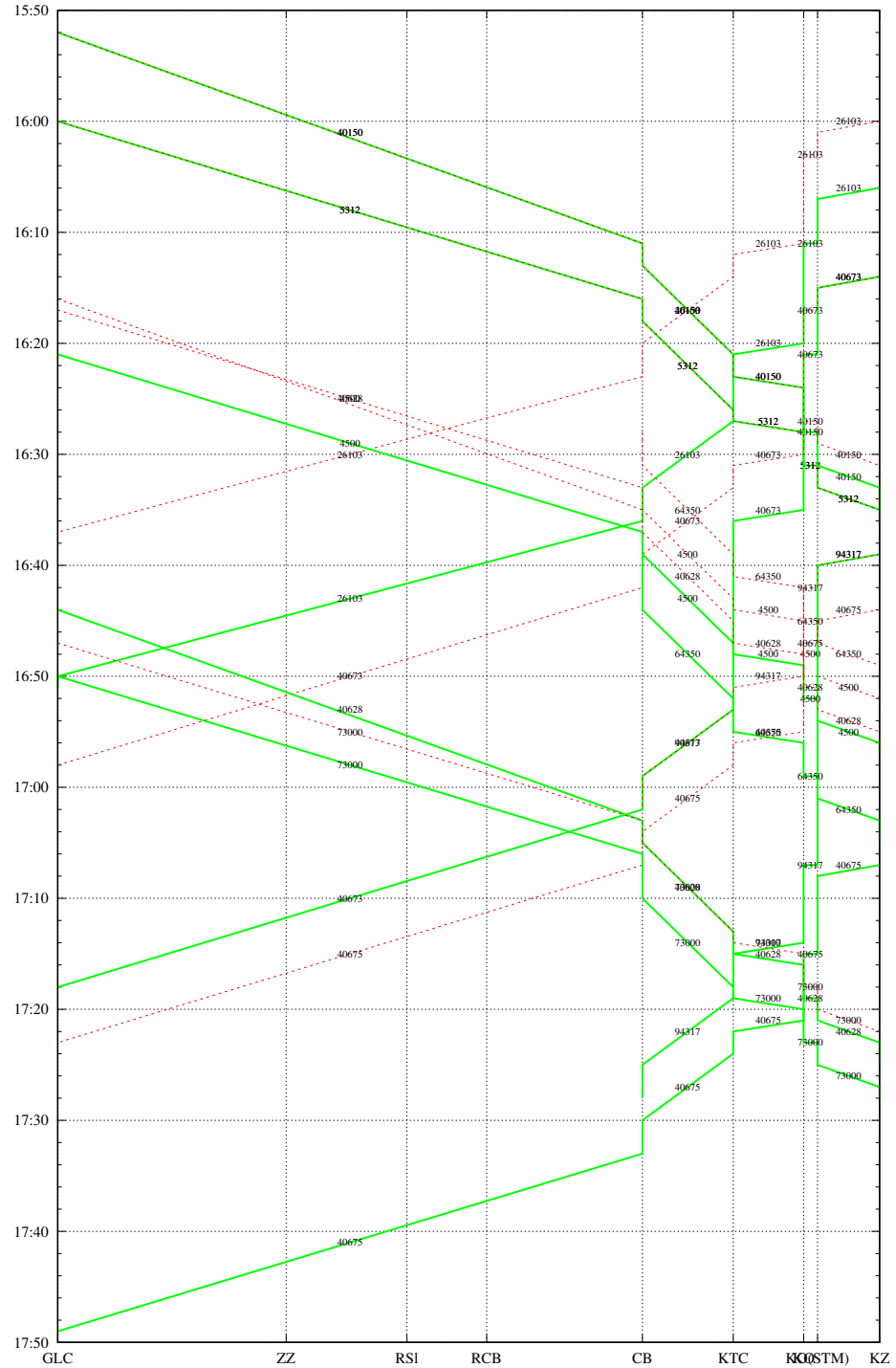


Fig. 8 Real-life experiment. Time-distance diagram CQM solution of network 7 (see Tab. 2) first realization. Closures (yielding single track line) are between CB and KTC as well as between KO(STM) and KZ.

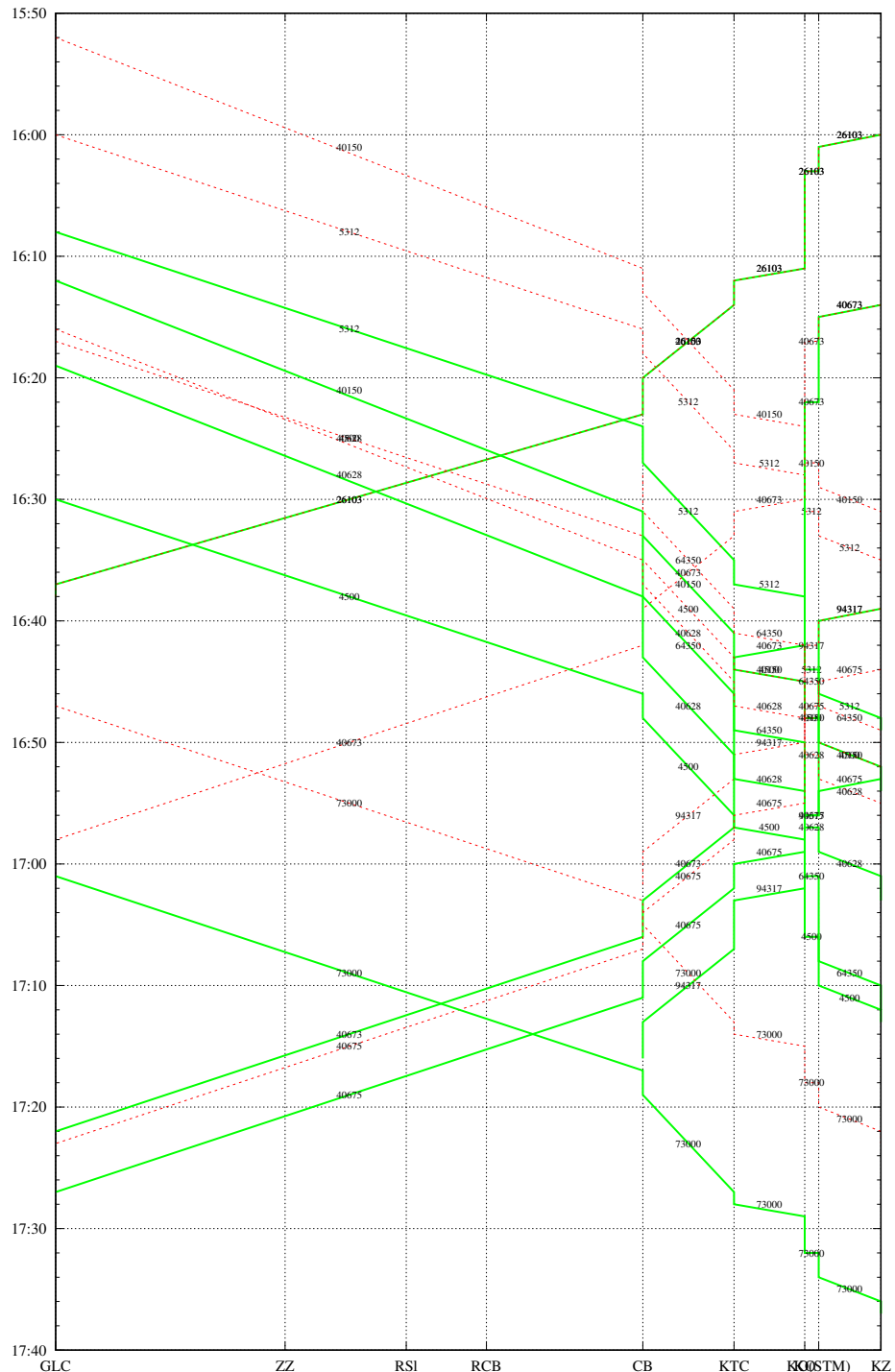


Fig. 9 Real-life experiment. Time-distance diagram CQM solution of network 7 (see Tab. 2) second realization.

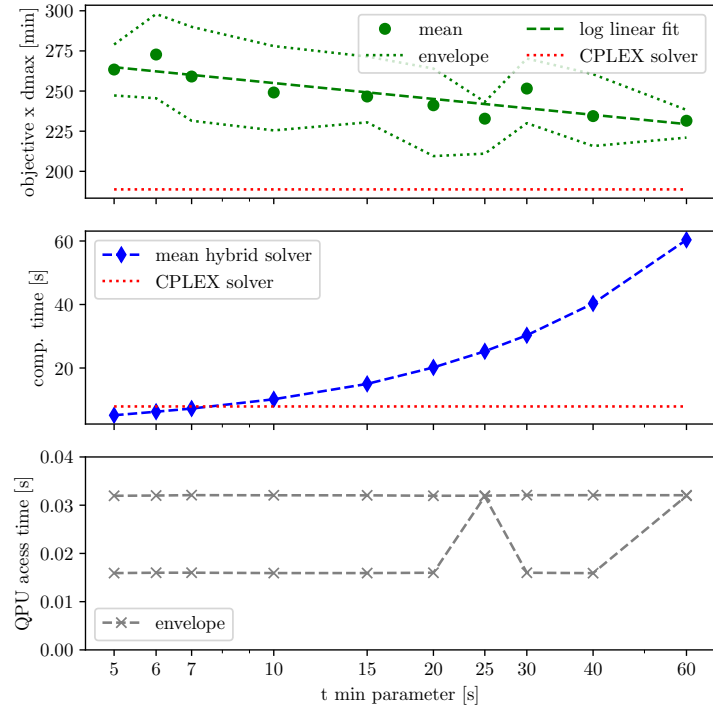


Fig. 10 Real-life experiments. The sweep over t_{min} parameter for network 7, see Tab. 2. All solutions were feasible. For higher t_{min} we expect smaller objective values but higher total computational time. For each parameter value there were 5 realizations of the experiment were performed. Interestingly, a linear (negatively sloped) relation between the objective and the logarithm of t_{min} can be observed, suggesting power law scaling.

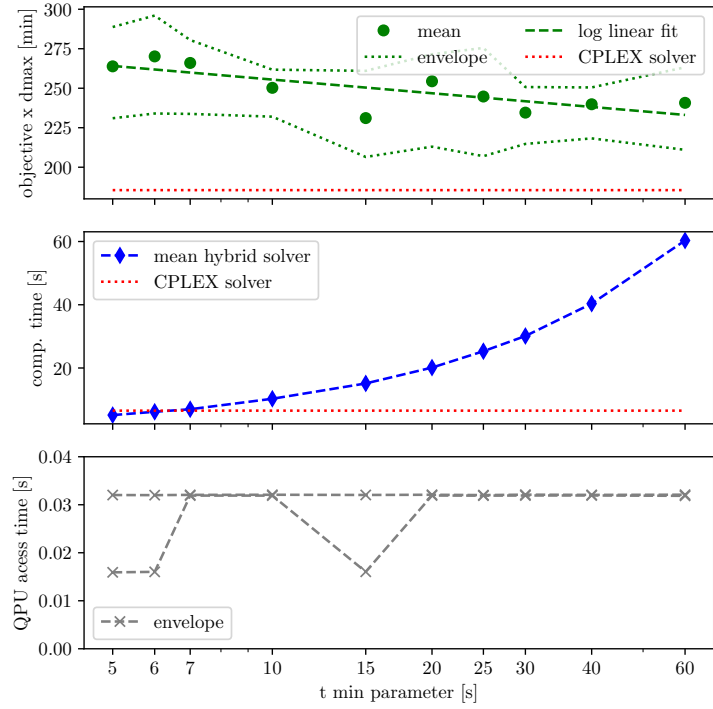


Fig. 11 Real-life experiments. The sweep over t_{\min} parameter for network 9, see Tab. 2. All solutions were feasible, results were similar to those in Fig. 10.